Advanced Modeling & Simulation (AMS) Seminar Series
NASA Ames Research Center
20 / 02 / 20

Massively Parallel Anisotropic Meshing Framework for CFD and Data Sciences

Elie Hachem, Aurélien Larcher, R. Valette

CFL | Computing and Fluids Research Group

CEMEF | MINES ParisTech | PSL Research Univeristy

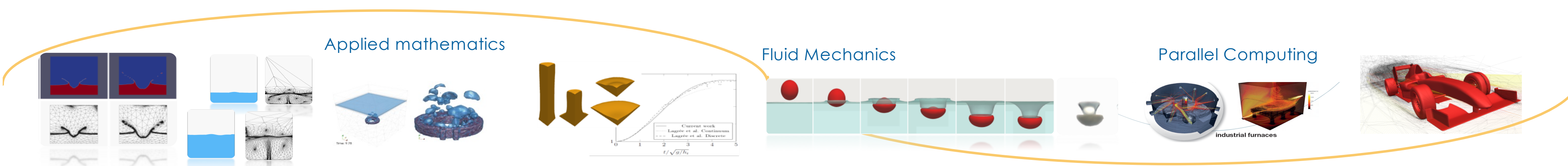

Outline & Objectives

1- Context and Motivation

2- Immersed method and Eulerian Framework

2- Anisotropic meshing with conservative interpolation

3- Stabilized FEM for complex fluids: turbulent flows, multiphase flows

4- Towards coupling CFD and Data Sciences

MINES ParisTech, PSL

- Founded in 1783
- 2300 persons, 240 researchers and professors, 400 PhDs
- 5 sites : Paris, Evry, Fontainebleau, Palaiseau and Sophia Antipolis
- 18 research centers
- 5 departments
  - Geosciences
  - Mathematics
  - Mechanics and Materials
  - Energy and Processes
  - Economy, management and Society

Paris

Sophia Antipolis

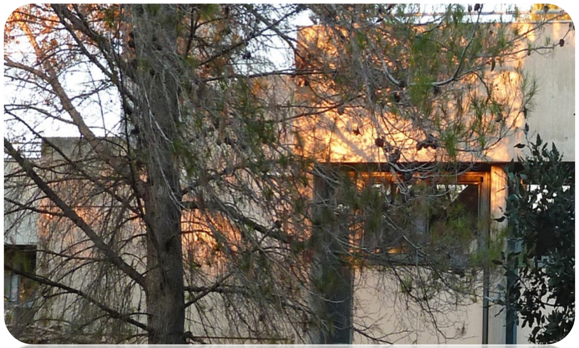

My office

CFL Computing and Fluids Research group

- 11 researchers and professors
- 19 PhDs and 3 Postdocs

Numerical framework (C++ parallel FEM library)

Applied Mathematics

- Unsteady Navier-Stokes equations
- Fluid-Structure interaction
- Turbulence and heat transfer
- Adjoint solution and control

Fluid Mechanics

- Multiphase flows (liquid, vapor, solid…)
- Yield stress and granular flows
- Darcy and Porous media
- Interface and surface tension

High Performance Computing

- Scalable implicit massively parallel solver
- A posteriori error estimator
- Anisotropic mesh adaptation

Challenges

« …essentially driven by real industrial applications »

Industrial Furnaces

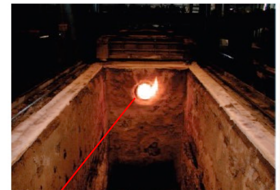

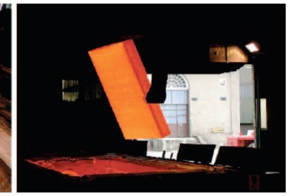

Heat Treatment

Burner at ~50m/s

Complex geometries

Turbulent mutliphase flows

Temperature > 1000° C

Quenching Process

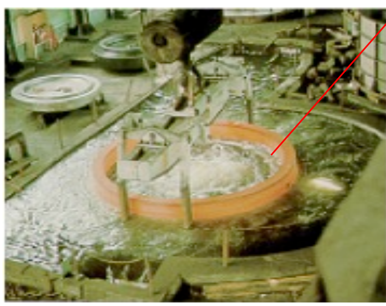

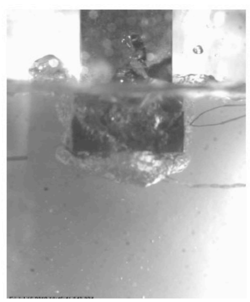

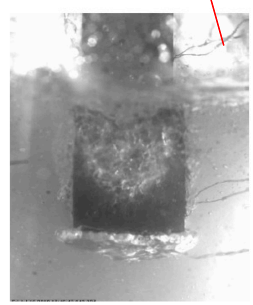

Metal Casting

Challenges

« …essentially driven by real industrial applications »

Involved physics
- Multiphase flows
- Turbulent boiling
- Phase change
- Liquid-gaz-solid flows
- Water “agitators”
- Surface tension
- High thermal gradients
-…

Process parameters:
- Orientation & position
- Size of the tank and the part
- Technology (jet, fall, …)
- Stirring devices
- Fluid (water, oil, polymer …)
- …

Other challenges

« …essentially driven by real industrial applications »

Jet impinging for cooling

Aerodynamic performance of a buckled wing drone

Design of a new stratospheric airship

Analysis and understanding of complex fluid flows

Eulerian approach

Common points:

- Complex geometries
- Different phases (fluid-fluid, fluid-solid, …)
- Need for optimization
- Accuracy at the interfaces
-Computational cost
-Repetitiveness
-…

Basic definition

$$\alpha(X) = \begin{cases} -\mathrm{dist}(X,\Gamma) \text{ if } X \in \Omega_1 \\ 0 \text{ if } X \in \Gamma \\ \mathrm{dist}(X,\Gamma) \text{ if } X \in \Omega_2 \end{cases}$$

- Transport equation $\frac{\partial \alpha}{\partial t} + u \cdot \nabla \alpha = 0$
- Hamilton-Jacobi problem $\frac{\partial \alpha}{\partial \tau} + s(\alpha)(\|\nabla \alpha\| - 1) = 0$

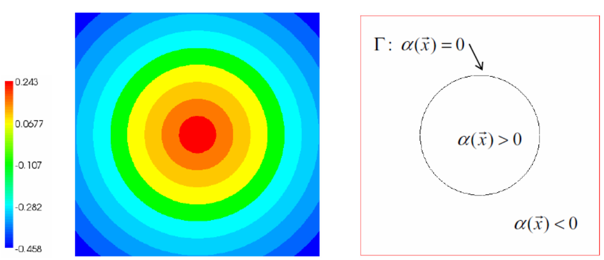

Shape representation

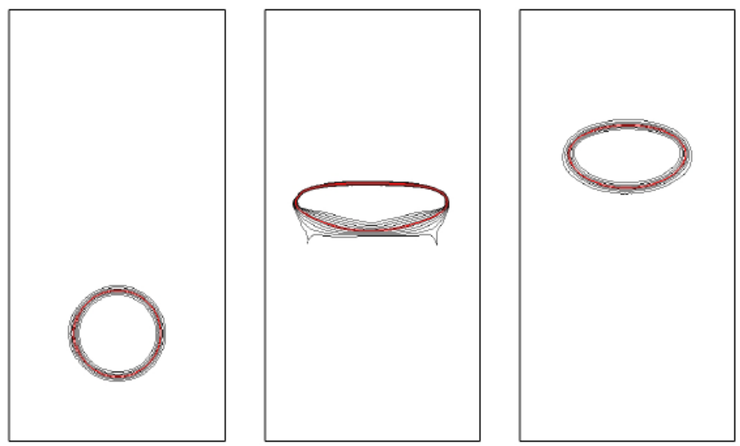

Rising bubble

Without re-distancing

With re-distancing

- × Frequency for redistancing
- × Mass conservation
- × Additional transport equation
- × Benefits from filtering
- × Benefits from stabilized FEM

$$s(\alpha) = \frac{\alpha}{\sqrt{\alpha^2 + \varepsilon^2}}$$

Interface capturing

- ❑ Apply a filter close to the interface, i.e. : $\tilde{\alpha} = \dfrac{1}{1+e^{-\frac{\alpha}{\varepsilon}}}$

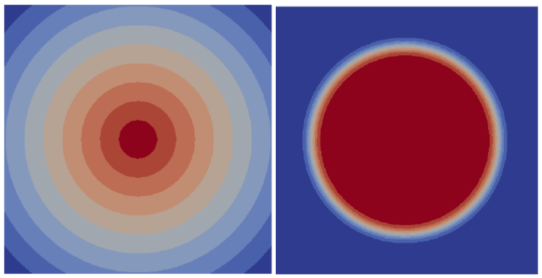

Regular and filtered level set function

- ❑ Auto re-initialization equation

$$\begin{cases} \dfrac{\partial \alpha}{\partial t} + u \cdot \nabla \alpha = 0 \\ \dfrac{\partial \alpha}{\partial \tau} + s(\alpha)(\|\nabla \alpha\| - 1) = 0 \end{cases}$$

- ❑ Shift the distance function restriction from α to $\tilde{\alpha}$

$$\|\nabla \alpha\| = 1 \quad \longrightarrow \quad \|\nabla \tilde{\alpha}\| = \frac{1}{\varepsilon}(1-\alpha)\alpha$$

- ❑ Convective reactive level set method

$$\frac{\partial \tilde{\alpha}}{\partial t} + (u + \underline{\lambda \mathrm{U}}) \cdot \nabla \tilde{\alpha} = s(\tilde{\alpha})\underline{\frac{\lambda}{\varepsilon}}(1-\tilde{\alpha})\tilde{\alpha}$$

- ❑ Time discretisation

$$\frac{3\tilde{\alpha}^{n+1} - 4\tilde{\alpha}^{n} + \tilde{\alpha}^{n-1}}{2\Delta t} + (u^{n+1} + \lambda \mathrm{U}^{n}) \cdot \nabla \tilde{\alpha}^{n+1} \underline{- s(\tilde{\alpha})\frac{\lambda}{\varepsilon}(1-\tilde{\alpha}^{n})\tilde{\alpha}^{n+1}} = 0$$

one choice among many for linearization

- ❑ Stabilized finite element variational formulation

$$\underline{\left(\frac{3\tilde{\alpha}_h^{n+1} - 4\tilde{\alpha}_h^{n} + \tilde{\alpha}_h^{n-1}}{2\Delta t}, \omega_h\right)_\Omega + ([u_h^{n+1} + \lambda \mathrm{U}_h^{n}] \cdot \nabla \tilde{\alpha}_h^{n+1}, \omega_h)_\Omega} - \left(\underline{s(\tilde{\alpha}_h)\frac{\lambda}{\varepsilon}(1-\tilde{\alpha}_h^{n})\tilde{\alpha}_h^{n+1}, \omega_h}\right)_\Omega$$

$$\underline{+ \sum_K (\mathscr{R}(\tilde{\alpha}_h^{n+1}), \tau^n [u_h^{n+1} + \lambda \mathrm{U}_h^{n}] \cdot \nabla \omega_h)_K + \sum_K (\mathscr{R}(\tilde{\alpha}_h^{n+1}), \tau^n \mid s(\tilde{\alpha}_h)\frac{\lambda}{\varepsilon}(1-\tilde{\alpha}_h^{n})\tilde{\alpha}_h^{n+1} \mid \cdot \omega_h)_K = 0,}$$

C.Bahbah, and , E.Hachem et. al, Conservative and adaptive level-set method for the simulation of two-fluid flows, Computers & Fluids, Vol 191, 2019

$$\mathscr{R} = \frac{\partial \tilde{\alpha}_h}{\partial t} - (u_h + \lambda \mathrm{U}_h \nabla \tilde{\alpha}_h) - s(\tilde{\alpha}_h)\frac{\lambda}{\varepsilon}(1-\tilde{\alpha}_h)\tilde{\alpha}_h$$

Illustration: collapse of a water column

- Two-fluid flow: water-air

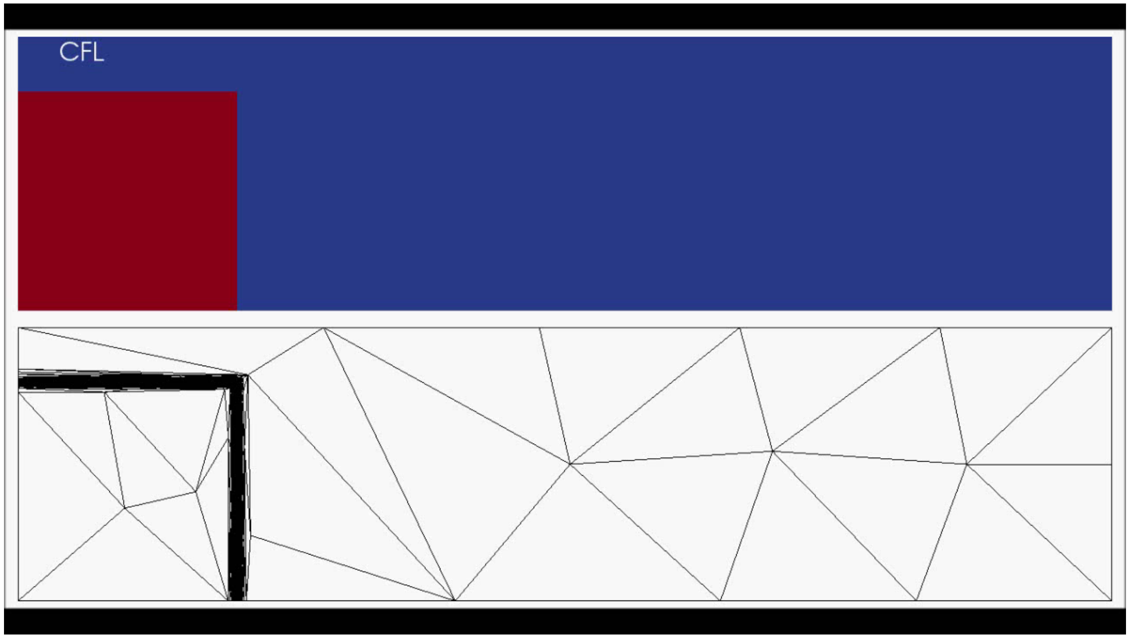

- Validation using 5000 nodes

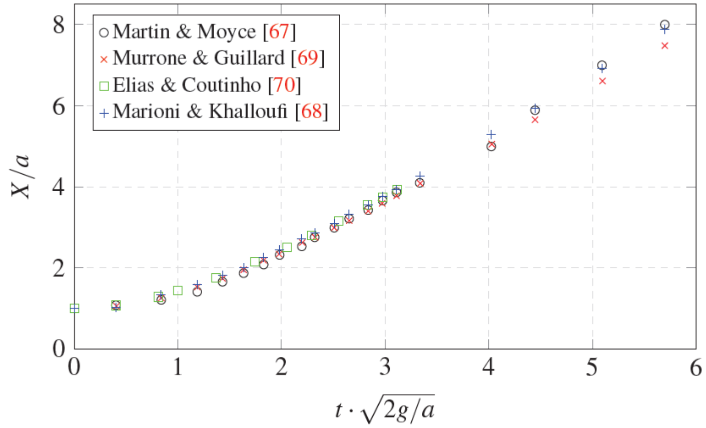

- Navier-Stokes ?
- Anisotropic meshing?
- Other physics (fluid-solid, complex fluids)?

M Khalloufi, Y Mesri, R Valette, E Massoni, E Hachem, High fidelity anisotropic adaptive variational multiscale method for multiphase flows with surface tension, Computer Methods in Applied Mechanics and Engineering, Vol 307, 44-67, 2016

L. Marioni, M. Khalloufi, F. Bay, E. Hachem, Two-fluid flow under the constraint of external magnetic field: revisiting the dam-break benchmark, International Journal of Numerical Methods for Heat & Fluid Flow, Vol. 27, pp. 2565-2581, 2017

The Navier-Stokes equations

VMS: Variational MultiScale

- VMS methods consider large scales which are defined by projection into appropriate spaces
- Models both velocity and pressure unresolved scales
- Similarity with the implicit version of LES

[T.J.R. Hugues et al.,1998]
[L.P. Franca, A. Nesliturk, 2001]
[R. Codina, 2002]
[V. Gravemeier, W.A. Wall, E. Ramm, 2004]
[A. Masud, R.A. Khurram, 2006]
[E. Hachem et al., 2010]
...

Variational Multiscale formulation: $\mathbf{v} = \mathbf{v}_h + \mathbf{v}'$ $\quad p = p_h + p'$

- the use of equal order continuous interpolations
- preventing from oscillations due to convection dominated flows

$$\text{find } (\mathbf{v}_h + \mathbf{v}', p_h + p') \in V_h \oplus V' \times P_h \oplus P' \text{ such that}$$

$$\begin{aligned}(\rho\delta_t(\mathbf{v}_h + \mathbf{v}'), \mathbf{w}_h + \mathbf{w}') + (\rho(\mathbf{v}_h + \mathbf{v}') \cdot \nabla(\mathbf{v}_h + \mathbf{v}'), \mathbf{w}_h + \mathbf{w}') - (p_h + p', \nabla\cdot(\mathbf{w}_h + \mathbf{w}'))& \\ +2(\eta\varepsilon(\mathbf{v}_h + \mathbf{v}'), \varepsilon(\mathbf{w}_h + \mathbf{w}')) = \langle \mathbf{f}, \mathbf{w}_h + \mathbf{w}' \rangle& \\ (q_h + q', \nabla \cdot (\mathbf{v}_h + \mathbf{v}')) = 0&\end{aligned}$$

$$\text{for all } (\mathbf{w}_h + \mathbf{w}', q_h + q') \in V_{h,0} \oplus V_0' \times P_{h,0} \oplus P_0'.$$

The subscales are approximated within each element K by:

$$\mathbf{v}' = \alpha_v \Pi_v'(\mathcal{R}_v), \quad p' = \alpha_p \Pi_p'(\mathcal{R}_p),$$

The Navier-Stokes equations

Variational MultiScale method:

- approximate the fine scale within each element *K*
- inserting the expressions of the subscales in the coarse scale equations
- fully implicit resolution

$$
\begin{aligned}
&(\rho\delta_t \mathbf{v}_h, \mathbf{w}_h) + (\rho\mathbf{v}_h \cdot \nabla\mathbf{v}_h, \mathbf{w}_h) - (p_h, \nabla \cdot \mathbf{w}_h) + 2(\eta\varepsilon(\mathbf{v}_h), \varepsilon(\mathbf{w}_h)) \\
&\quad + \sum_K \alpha_v(\rho\delta_t\mathbf{v}_h + \rho\mathbf{v}_h \cdot \nabla\mathbf{v}_h + \nabla p_h - \nabla\cdot(2\eta\varepsilon(\mathbf{v}_h)), \rho\mathbf{v}_h\cdot\nabla\mathbf{w}_h + \nabla\cdot(2\eta\varepsilon(\mathbf{w}_h)))_K \\
&\quad + \sum_K \alpha_p(\nabla\cdot\mathbf{v}_h, \nabla\cdot\mathbf{w}_h) \\
&\quad = \langle \mathbf{f}, \mathbf{w}_h\rangle + \sum_K \alpha_v(\mathbf{f}, \rho\mathbf{v}_h\cdot\nabla\mathbf{w}_h + 2\eta\nabla\cdot\varepsilon(\mathbf{w}_h))_K \\
&(q_h, \nabla\cdot\mathbf{v}_h) + \sum_K \alpha_v(\rho\delta_t\mathbf{v}_h + \rho\mathbf{v}_h\cdot\nabla\mathbf{v}_h + \nabla p_h - \nabla\cdot(2\eta\varepsilon(\mathbf{v}_h)), \nabla q_h)_K \\
&\quad = \sum_K \alpha_v(\mathbf{f}, \nabla q_h)_K
\end{aligned}
\tag{2.24}
$$

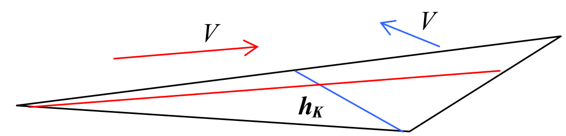

and the stabilization parameters:

$$
\alpha_v = \left[\left(\frac{c_1\eta}{\rho h^2}\right)^2 + \left(\frac{c_2\|\mathbf{v}_h\|_K}{h}\right)^2\right]^{-1/2} \qquad \alpha_p = \left[\left(\frac{\eta}{\rho}\right)^2 + \left(\frac{c_2\|\mathbf{v}_h\|_K h}{c_1}\right)^2\right]^{1/2} \qquad h_K = \frac{2|\mathbf{v}_h|}{\Sigma_{i=1}^{N_K}|\mathbf{v}_h\cdot\nabla\varphi_i|}
$$

[E. Hachem *et. al*, JCP 2010]
[E. Hachem *et. al*, CMAME, 2016]
[P. Meliga & E. Hachem, JCP, 2018]

Anisotropic meshing

❑ Metric-based anisotropic mesh adaptation

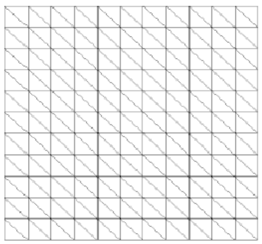

$$+ \; M = \begin{pmatrix} \frac{1}{0.01^2} & \\ & \frac{1}{1^2} \end{pmatrix} \longrightarrow$$

Metric (directions, size)

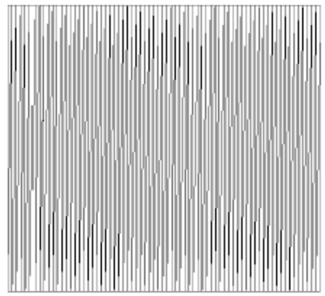

❑ Motivation 1

- Enables to capture scale heterogeneities
- Enables to deal with discontinuities or gradients
- Crucial for boundary layers, shock waves, …
- Crucial for complex geometry: curvature, sharp angles,…

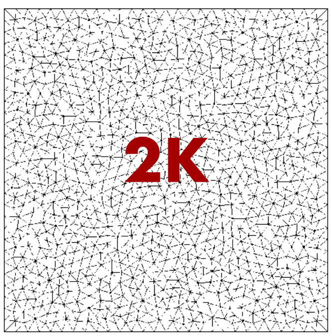

vs

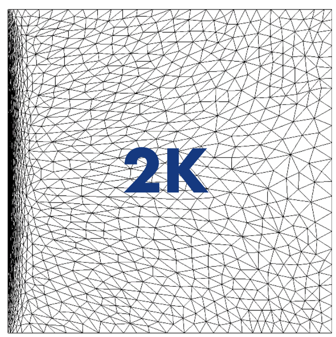

❑ Motivation 2

- Dynamic Mesh adaptation
- A posteriori error estimator
- Multi criteria adaptation
- Control (i.e. number of elements)
- Error analysis

P. J. Frey and F. Alauzet. Anisotropic mesh adaptation for cfd computations. Computer Methods in Applied Mechanics and Engineering, 194(48-49):5068–5082, 2005.
J.-F. Remacle, X. Li, M.S. Shephard, and J.E. Flaherty. Anisotropic adaptive simulation of transient flows. International Journal for Numerical Methods in Engineering, 62:899–923, 2005
H. Beaugendrea R. Abgrall and C. Dobrzynskia. An immersed boundary method using unstructured anisotropic mesh adaptation combined with level-sets and penalization techniques. Journal of Computational Physics, 257:83–101, 2014

Combining mesh adaptation with SFEM

- Metric construction $\widetilde{\mathbb{M}}^i = \frac{|\Gamma(i)|}{d}\left(\widetilde{\mathbb{X}}^i\right)^{-1}$

  - Candidate for directions:

$$\mathbb{X}^i = \frac{d}{|\Gamma(i)|}\sum_{j\in\Gamma(i)} \mathbf{X}^{ij}\otimes\mathbf{X}^{ij}$$

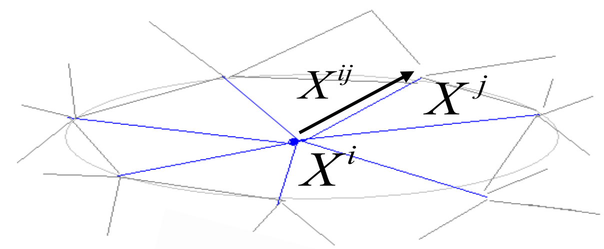

  - Control the size of each edge X^{ij} using a stretching factor:

$$\widetilde{\mathbf{X}^{ij}} = s_{ij}\mathbf{X}^{ij}$$

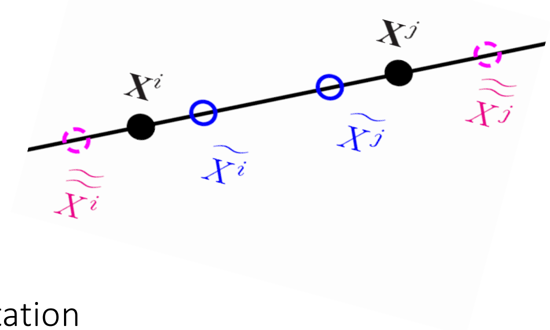

  - Drive these stretching factors using an edge based error estimator:

  - Multi criteria mesh adaptation

$$s_{ij} = \left(\frac{e}{e(N)}\right)^{-\frac{1}{2}} = \left(\frac{\sum_i n^i(1)}{N}\right)^{\frac{2}{d}} e_{ij}^{-1/2}$$

$$\mathbf{v}(\mathbf{x}^i) = \left\{\frac{\hat{\alpha}}{E}, \frac{v^i}{||v^i||}, \frac{||v^i||}{\max_j ||v^j||}, \frac{\eta_{eff}}{\max(\eta_{eff})}\right\}$$

T. Coupez, E. Hachem, Solution of high-Reynolds incompressible flow with stabilized finite element and adaptive anisotropic meshing, Computer methods in applied mechanics and engineering, Vol. 267, 65-85, 2013

Revisiting the lid driven cavity

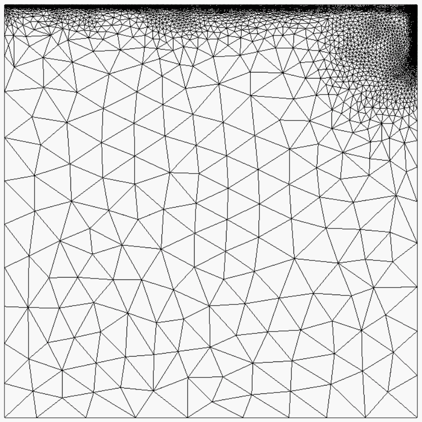

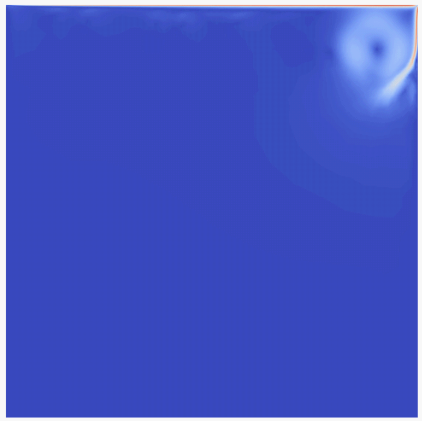

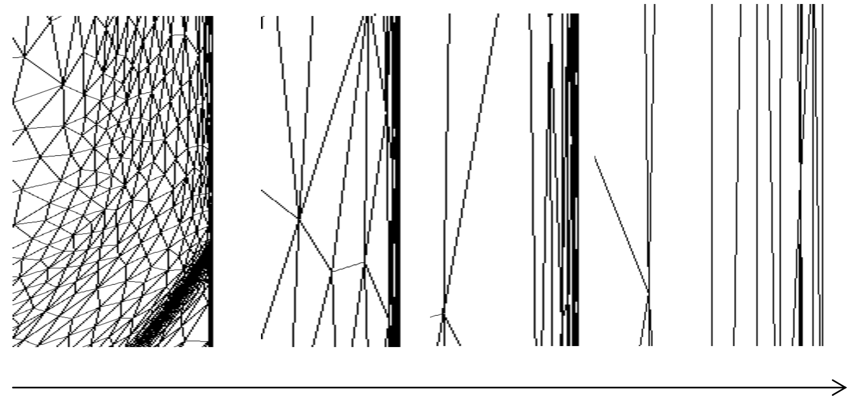

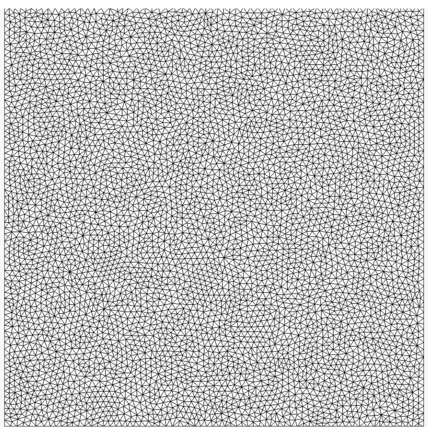

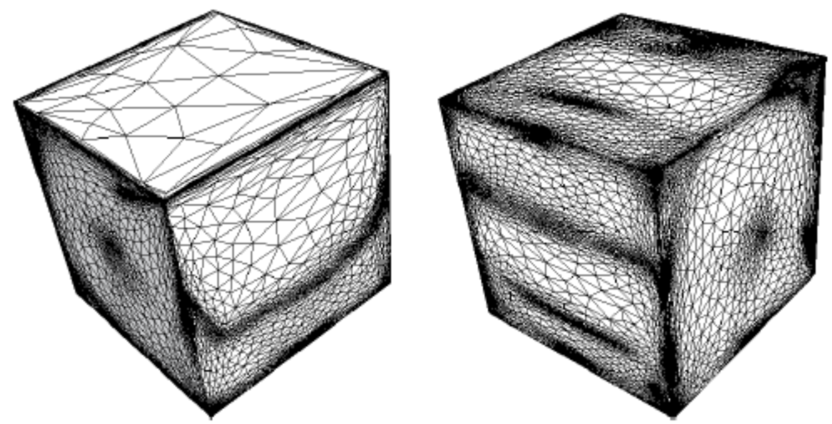

Combining **BLM** (boundary layer metric) and **EBM** (edge-based metric)

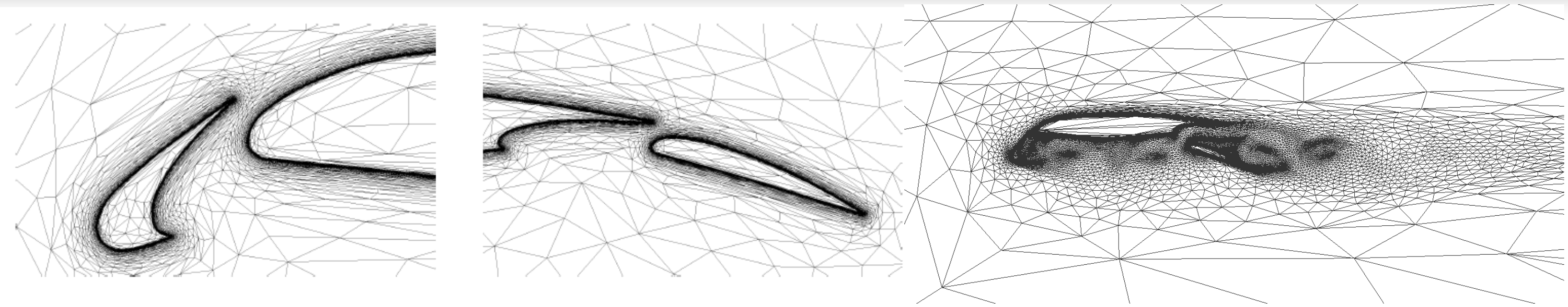

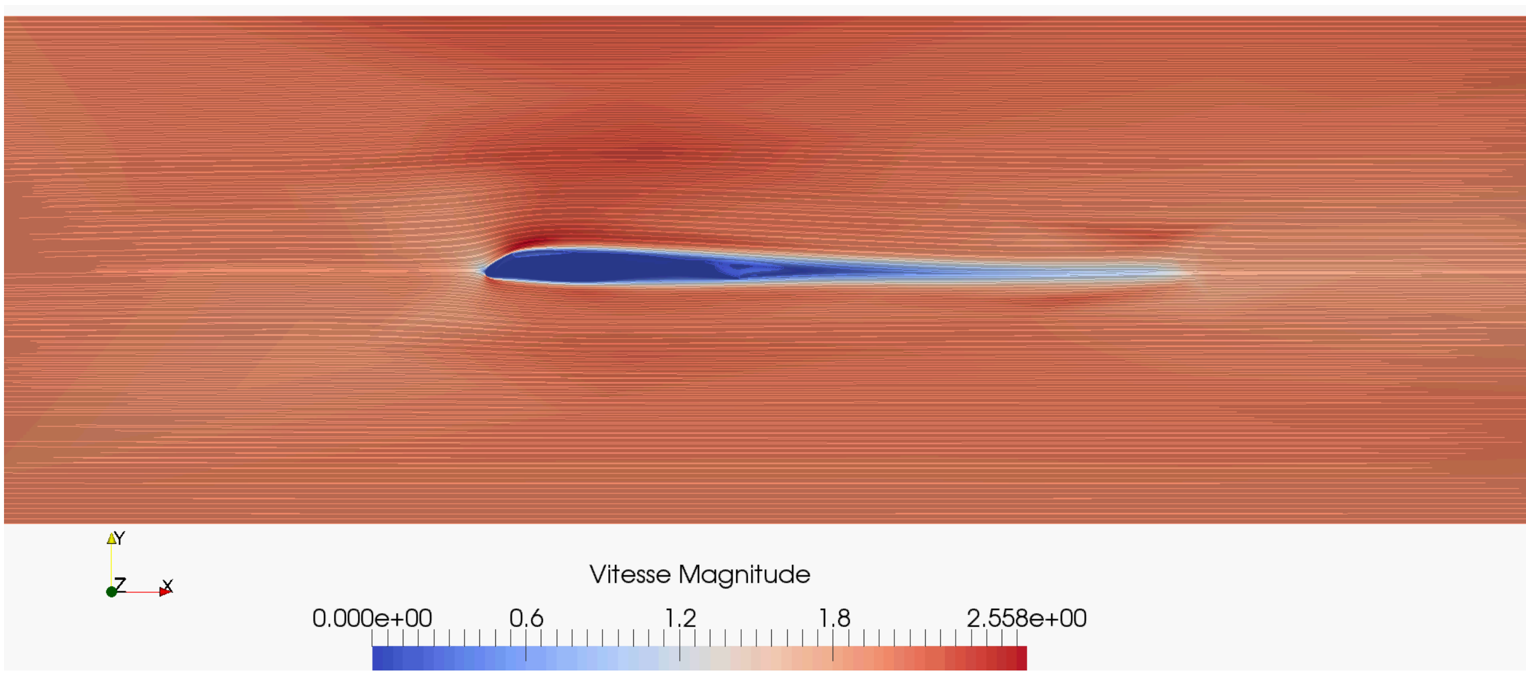

Optimal control of each sub-layer

Multi-levelset framework

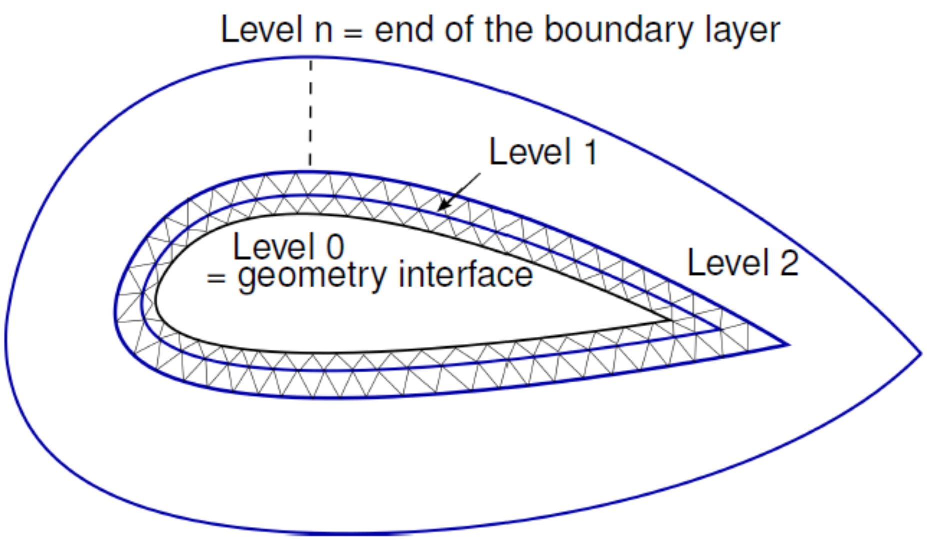

$$\text{Levels}[k] = \text{Levels}[k-1] + h_{\min} \times \alpha^{k-1} = \text{Levels}[0] + h_{\min}(1-\alpha^k)/(1-\alpha)$$

$$\mathsf{M} = \frac{1}{h_n^2}\mathbf{N} \times \mathbf{N}^{\mathbf{T}} + \frac{1}{h_t^2}(\mathsf{I_d} - \mathbf{N} \times \mathbf{N}^{\mathbf{T}})$$

- Tangential mesh size must depend on the geometry and consequently:
  → shape, curvature and the complexity of the geometry

- In three dimensions, the geometry can have different behavior in its two tangential directions.

  ✓ We refer to the geometry curvature to define properly the tangential directions and associated mesh sizes

  ✓ It will allow us to define properly the anisotropic ratio and to ensure that the interface is smoothly and well described.

L. Billon, Y. Mesri, E. Hachem, Anisotropic boundary layer mesh generation for immersed complex geometries, Engineering with Computers, pp. 1-12, 2016

Optimal control of each sub-layer

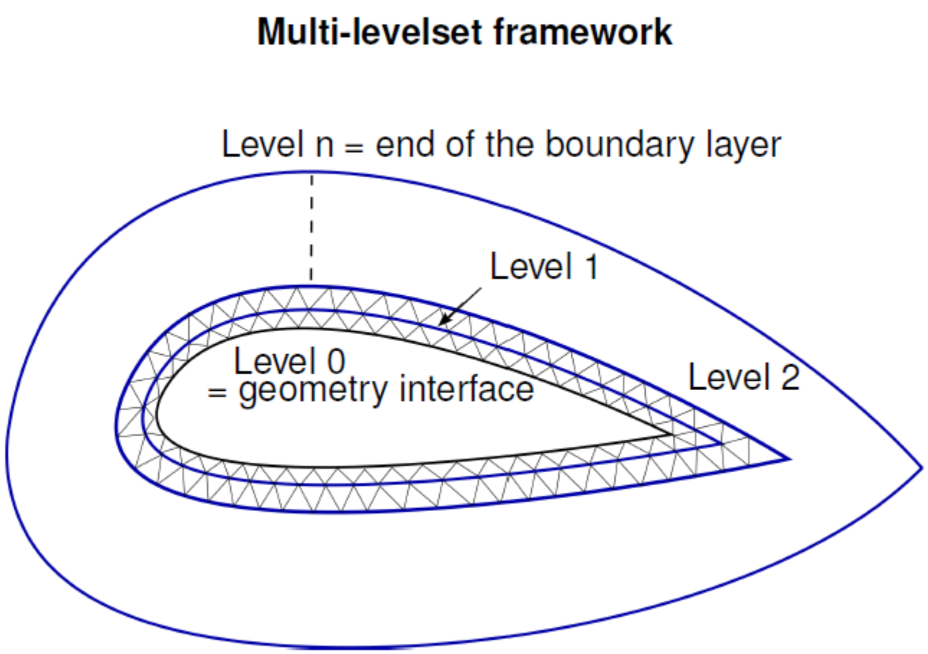

$$
\begin{aligned}
\text{Levels}[k] &= \text{Levels}[k-1] + h_{\min} \times \alpha^{k-1} \\
&= \text{Levels}[0] + h_{\min}(1-\alpha^k)/(1-\alpha)
\end{aligned}
$$

- Boundary layer at the geometry interface
- Ensure a smooth mesh size transition
- Build a quasi-structured mesh at the interface

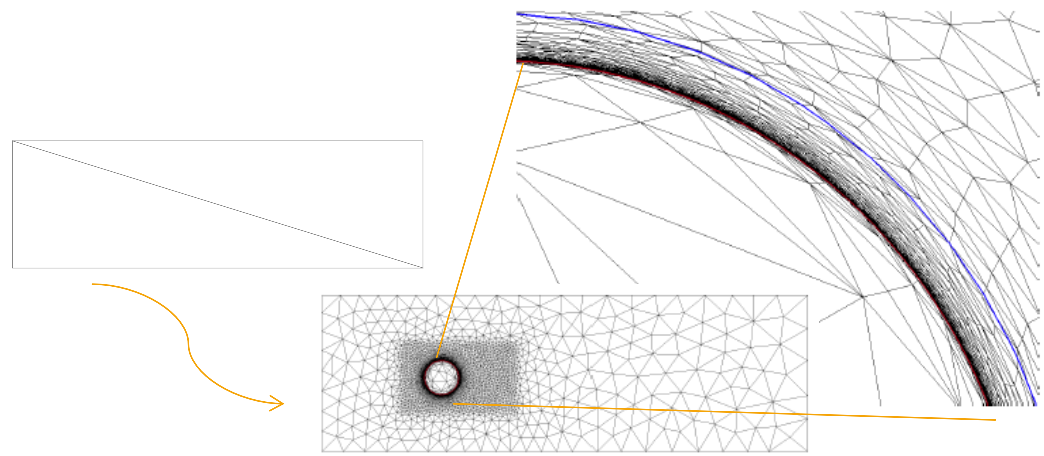

L. Billon, Y. Mesri, E. Hachem, Anisotropic boundary layer mesh generation for immersed complex geometries, Engineering with Computers, pp. 1-12, 2016

BLM (boundary layer metric)

NACA0012: $\mathrm{Re} = 6 \cdot 10^6$

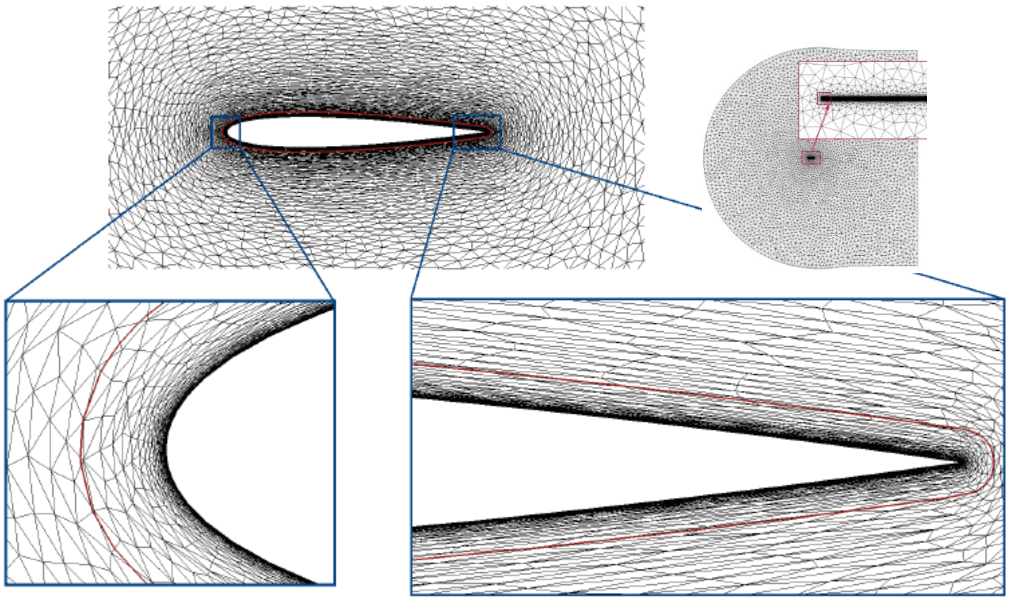

$y_0^+ = 1,\ h_{\min} = 4.46 \cdot 10^{-6}$

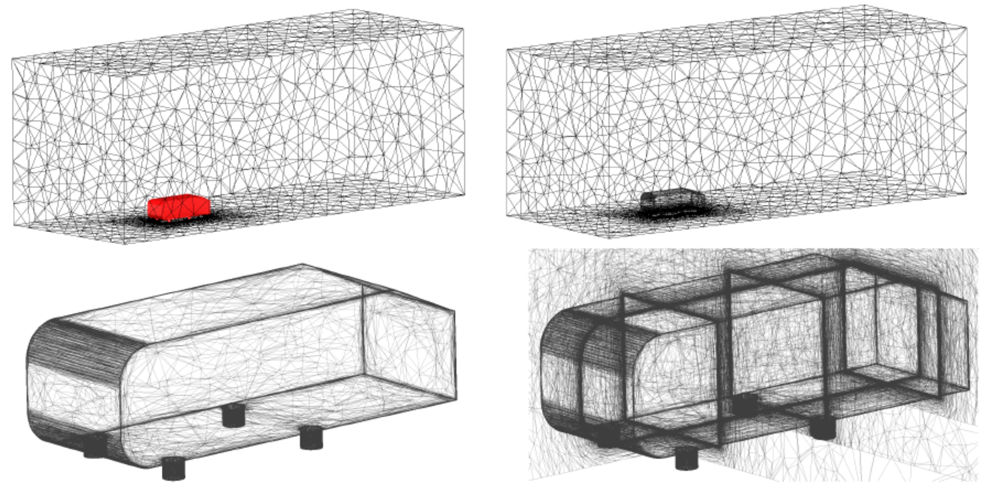

2.167.057 elements - 378.259 nodes - 20 cores

$\mathrm{Re} = 4.25 \cdot 10^6$ - $h_{\min} = 3 \cdot 10^{-4}$

G. Guiza, A. Larcher, A. Goetz, L. Billon, P. Meliga, E. Hachem, Anisotropic boundary layer mesh generation for reliable 3D unsteady RANS simulations, Finite Elements in Analysis and Design 170, 103345

BLM (boundary layer metric)

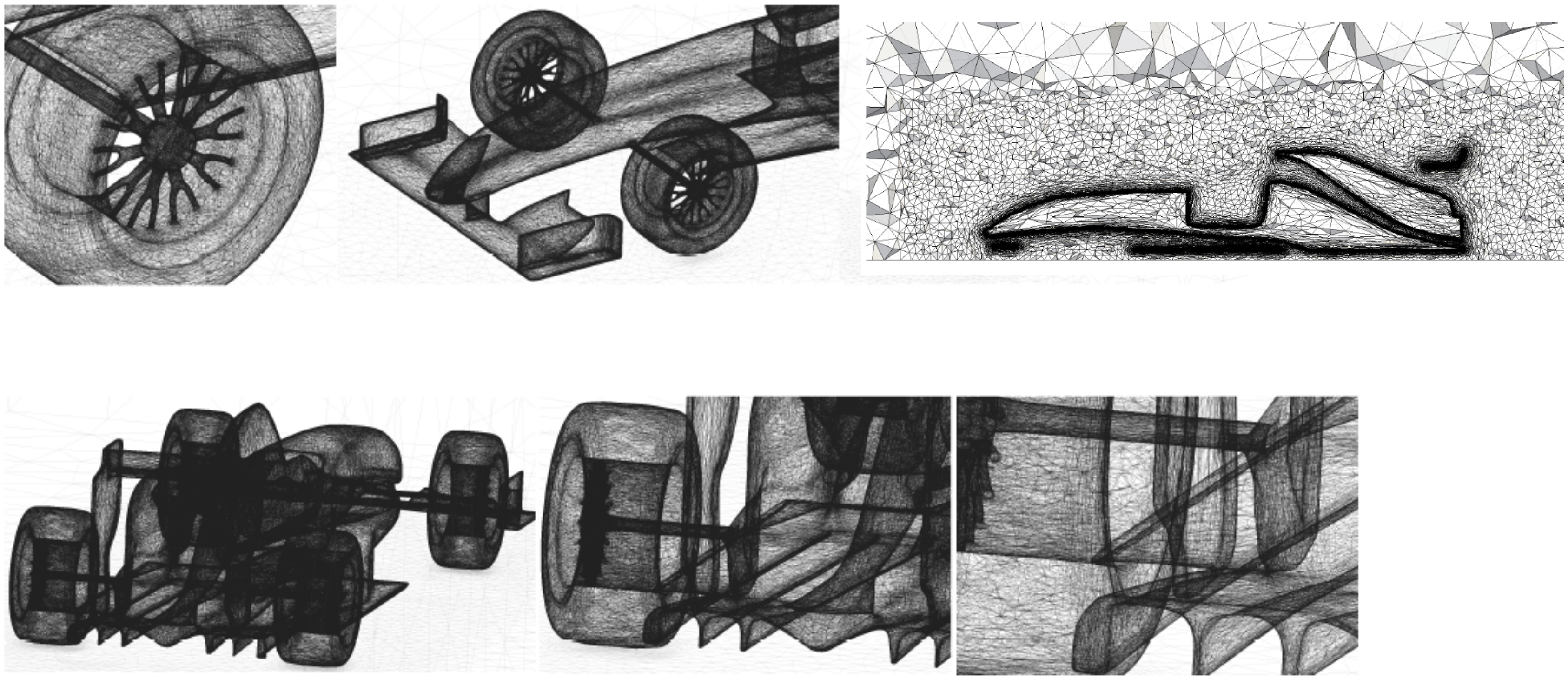

21.026.520 elements - 3.602.483 nodes - 40 cores

$\mathrm{Re} = 2 \cdot 10^{7}$ - $h_{\min} = 6 \cdot 10^{-4}$

BLM (boundary layer metric)

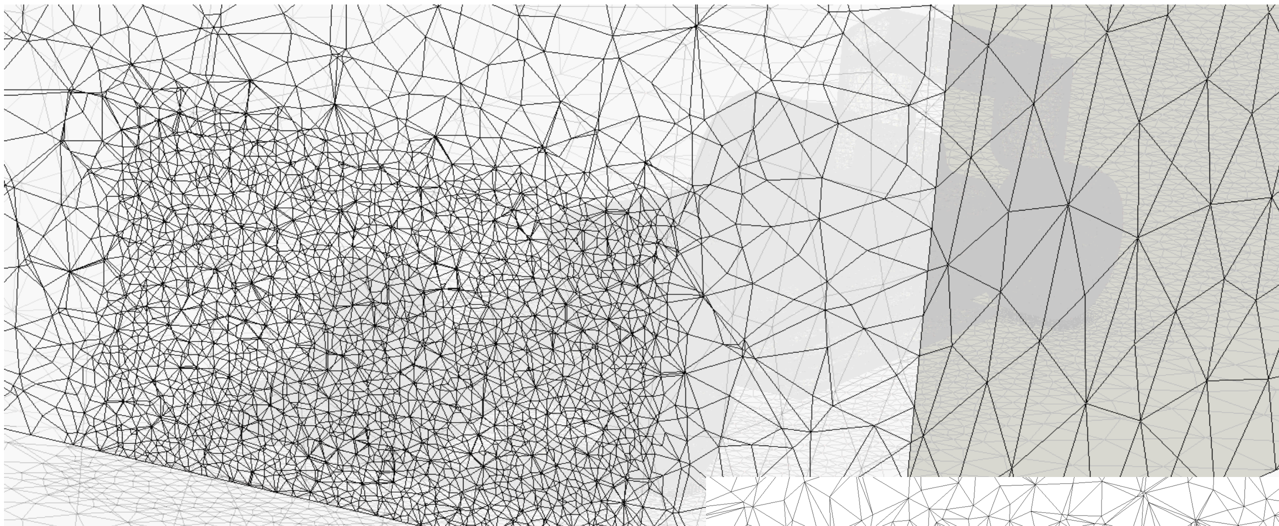

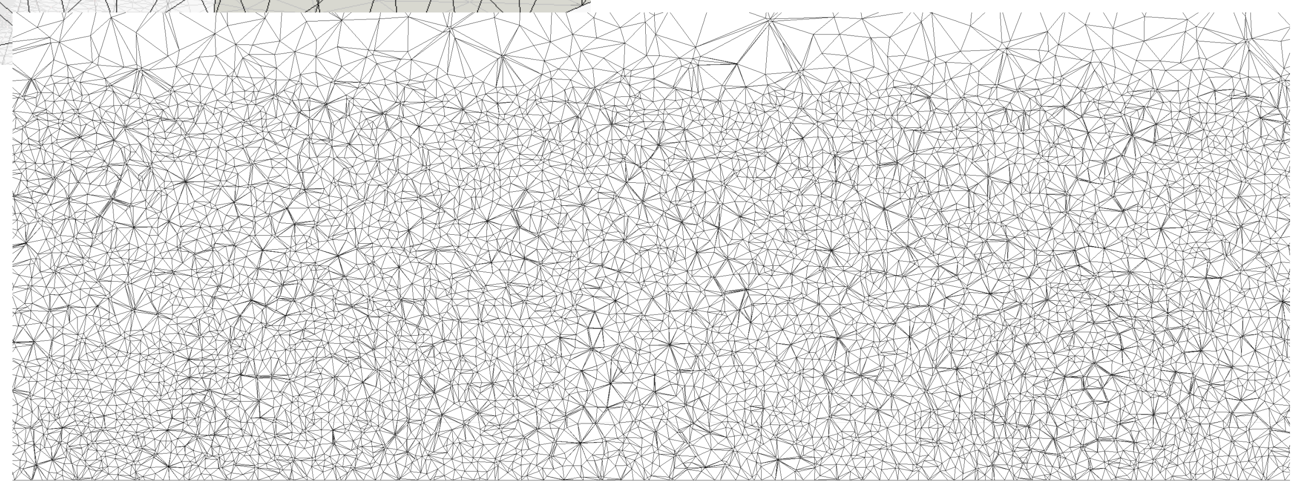

An iterative process – immersed of complex geometries

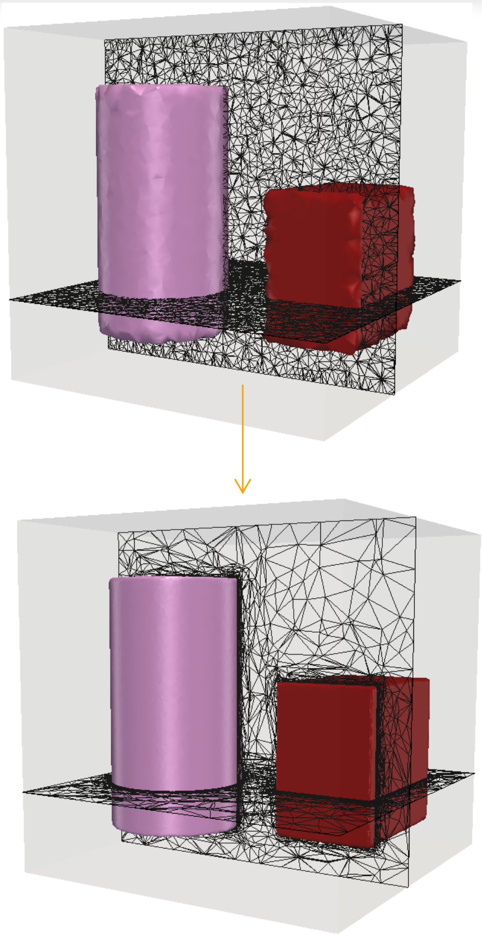

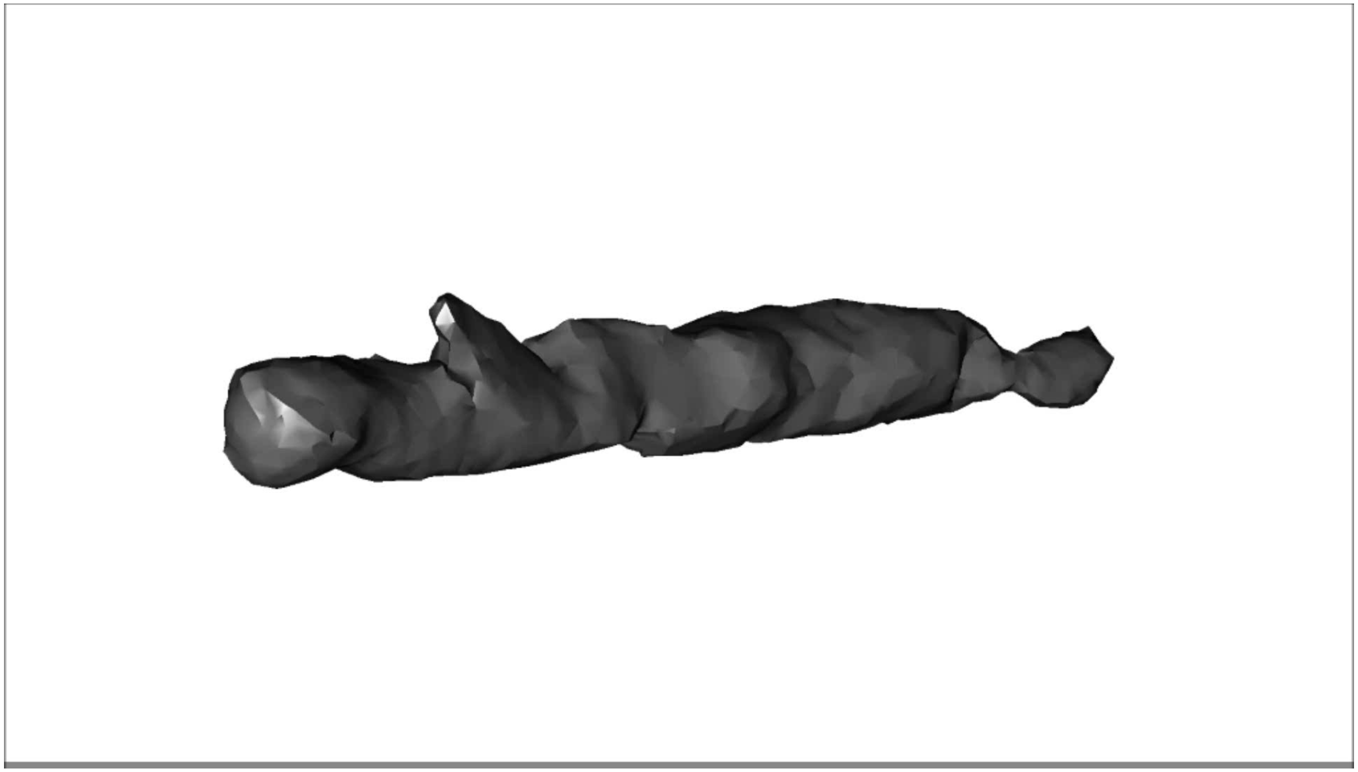

Isovalues of the distance function on an anisotropic mesh

Towards a general Eulerian two-fluid framework

Liquid-vapor flows

Yield stress flows

Granular flows

Eulerian two-fluid framework

Continuum approach for granular flow

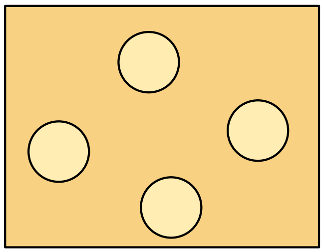

liquid

→ Newtonian behaviour

Newtonian

$$\tau = 2\eta D(u)$$

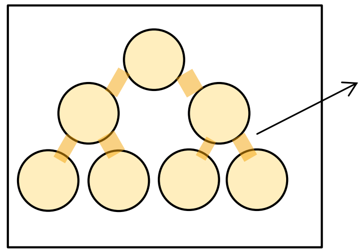

Intermediate state

→ Yield stress fluid

Bingham

$$\tau = \left(2\eta + \frac{\tau_0}{\dot{\gamma}}\right) D(u)$$

$$\dot{\gamma} = \| D(u) \|$$

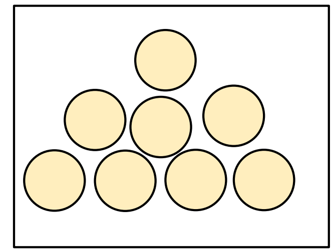

Granular material

→ Pressure-dependent behaviour

Granular

$$\tau = 2\left(\frac{\mu - \mu_s}{I + I_0} I + \frac{\mu_s}{\dot{\gamma}}\right) p D(u)$$

Jop et al., Nature, 2006

Numerical issues

$p \rightarrow 0$ $\dot{\gamma} \rightarrow 0$ surface tension high density / viscosity ratios

Coupling with fluid mechanics

Surface tension

$$\Delta t < (\Delta x)^{\frac{3}{2}} \sqrt{\frac{\bar{\rho}}{2\pi\gamma}}$$

$$f_{\mathrm{ST}} = -\gamma\kappa\delta(\alpha)\mathrm{n} - \gamma\delta(\alpha)\Delta t \left(\frac{\partial^2 \mathrm{u}}{\partial \mathrm{n}^2} + \kappa \frac{\partial \mathrm{u}}{\partial \mathrm{n}} - \nabla^2 \mathrm{u}^{n+1}\right)$$

M. Khalloufi, Y. Mesri, R. Valette, E. Hachem, CMAME 2016

Papanastasiou regularization method

[T. Papanastasiou 1987]

$$\eta_{eff} = \eta_p + \frac{\tau_0}{\dot{\bar{\varepsilon}}}[1 - exp(-m\dot{\bar{\varepsilon}})]$$

m : Papanastasiou regularization coefficient

S. Riber, Y. Mesri, R. Valette, E. Hachem, Computers & Fluids, 2016

Extended to 3D free surface flows

[M. Bercovier,1980]

$$\eta_{eff} = min\left(\eta_{air}, \eta_f(p, ||\dot{\gamma}||) + \frac{\tau_0(p)}{\sqrt{||\dot{\gamma}||^2 + ||\dot{\gamma}||^2_{min}}}\right)$$

R. Valette, S. Riber, A.S. Pereira, M. Khalloufi, L. Sardo, E. Hachem, J. Comp. Phys., submit 2018

Numerical test 1: rising bubble

(a) t=0.6s (b) t=1.2s (c) t=1.8s (d) t=2.2s

(e) t=2.4s (f) t=2.6s (g) t=2.8s (h) t=3.0s

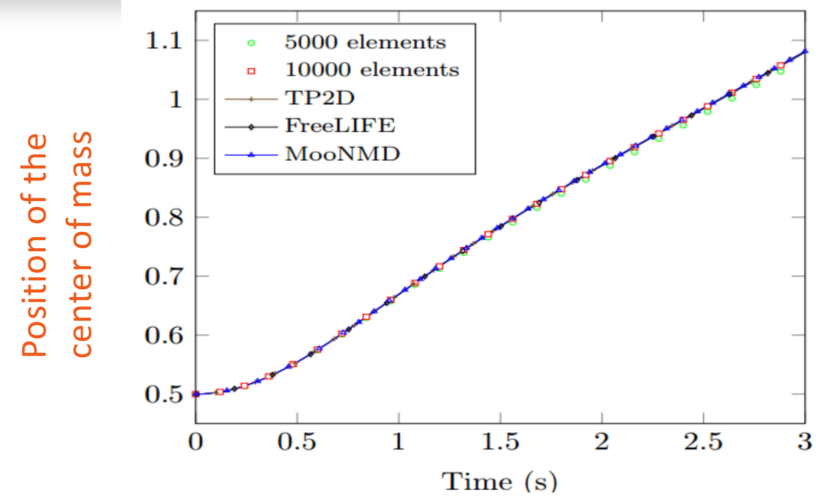

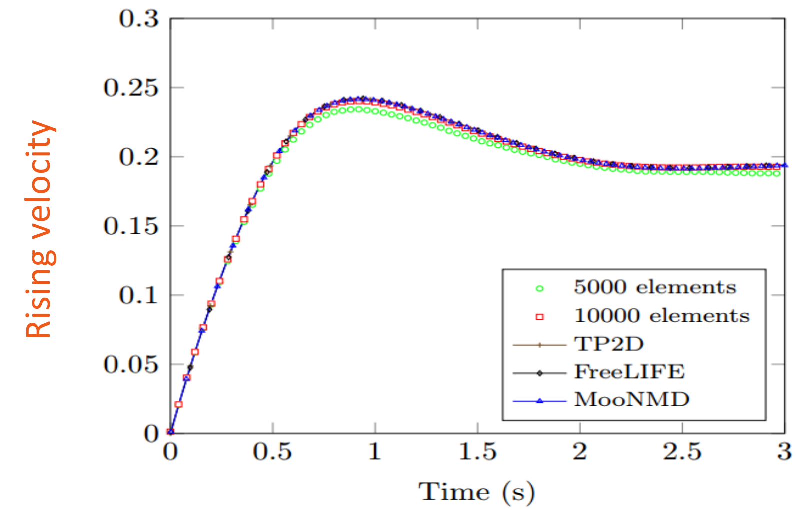

Numerical test 2: collapse of a granular column

- 3D dam break

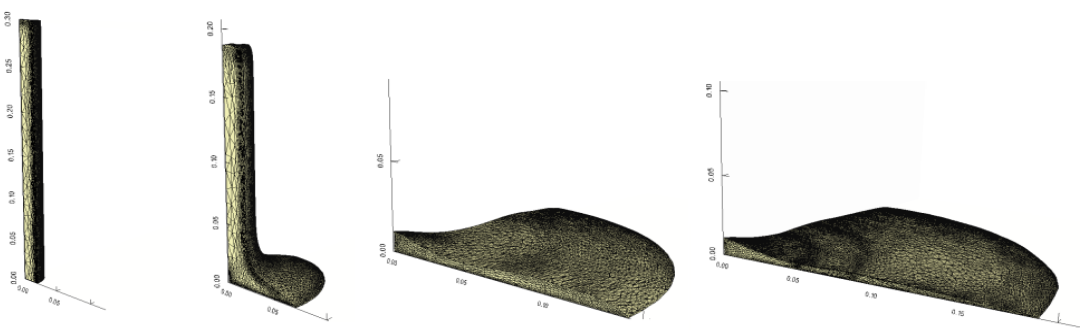

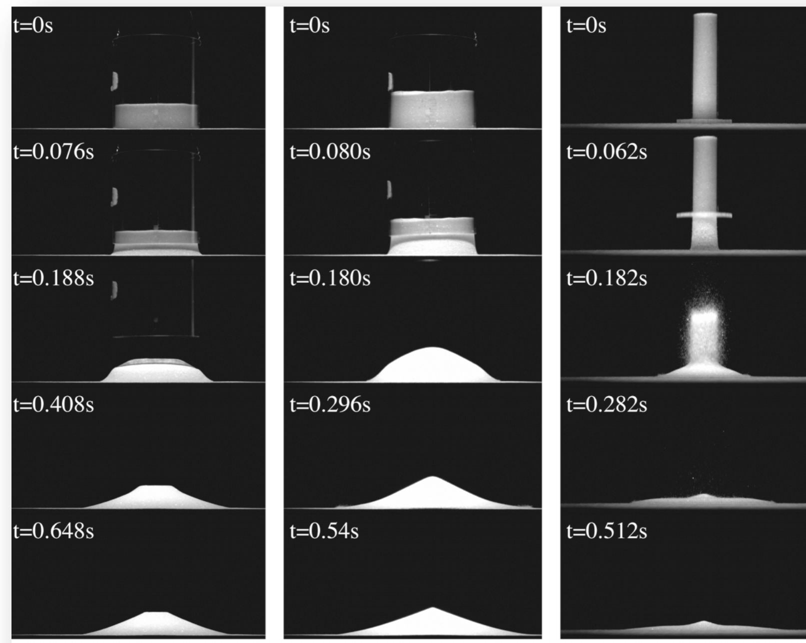

(a) (b) (c)

R. Valette, S Riber, L Sardo, R Castellani, F Costes, N Vriend, E Hachem, Sensitivity to the rheology and geometry of granular collapses by using the μ (I) rheology, Computers & Fluids 191, 104260

Numerical test 2: collapse of a granular column

- Comparisons with the discrete method

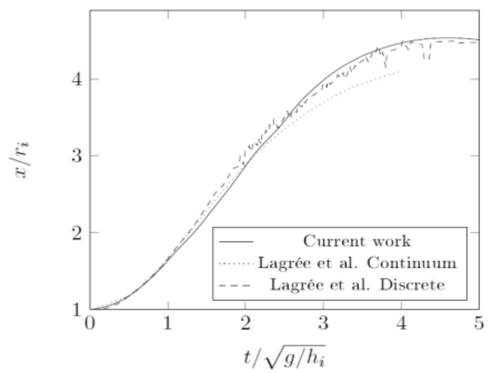

(b) $a = 1.42$

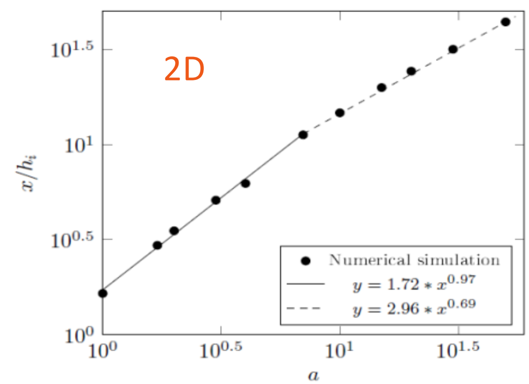

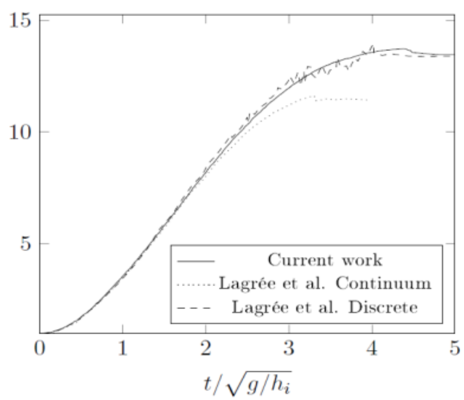

(c) $a = 6.26$

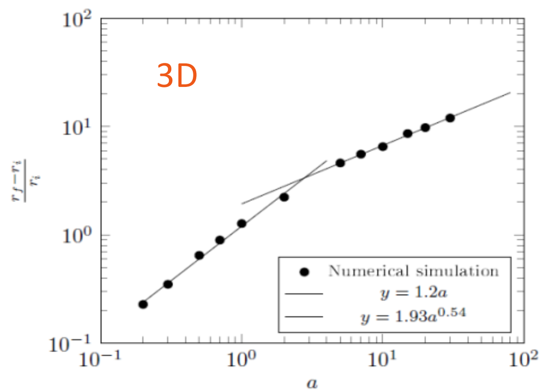

Lagree et al., J. Fluid Mech. 2011

Aspect ratio a=2

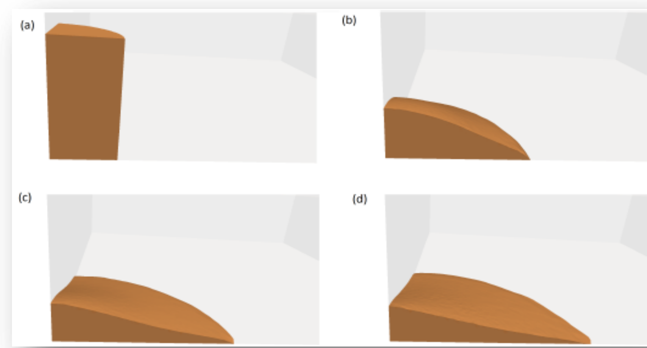

Aspect ratio a=7

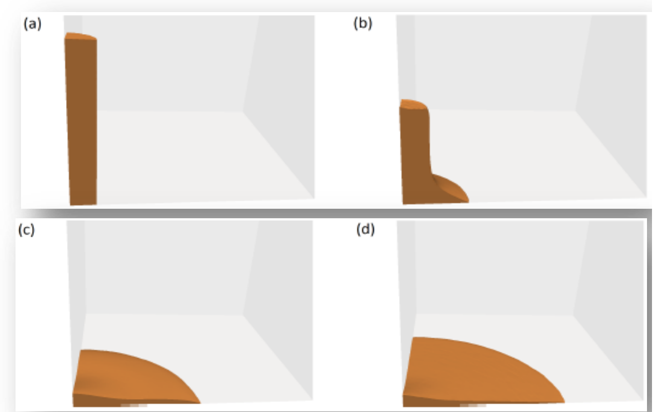

Numerical test 3: Collapse of a Bingham column

- 2D and 3D Bingham dam break problem: effective viscosity, yielded regions and adapted mesh

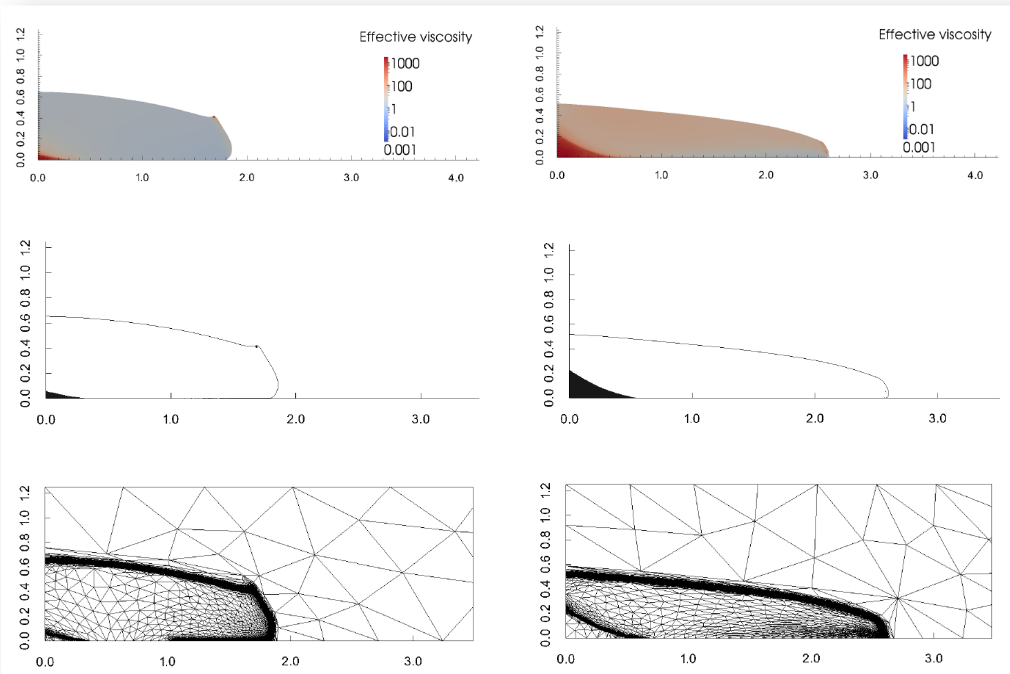

Aspect ratio a = 1
Bn = 0:03 at
t = 10 and 100

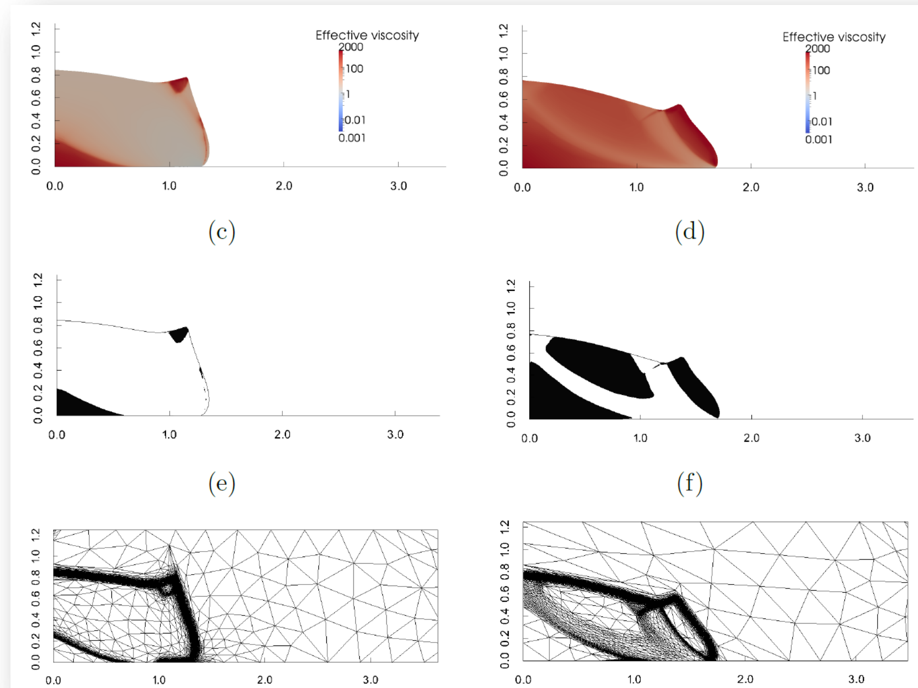

Aspect ratio a = 1
Bn = 0:1
t = 10 and 100

Numerical test 3: Collapse of a Bingham column (new benchmark)

- 2D and 3D Bingham dam break problem: effective viscosity, yielded regions and adapted mesh

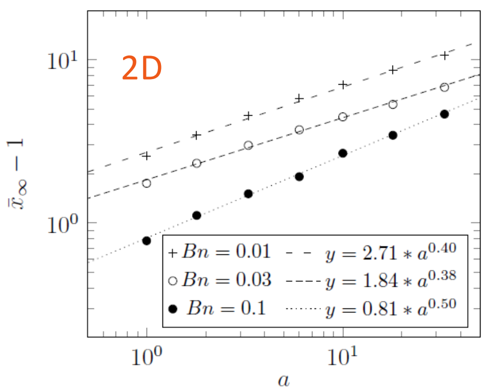

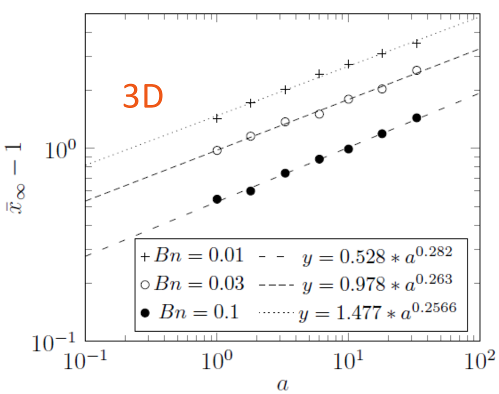

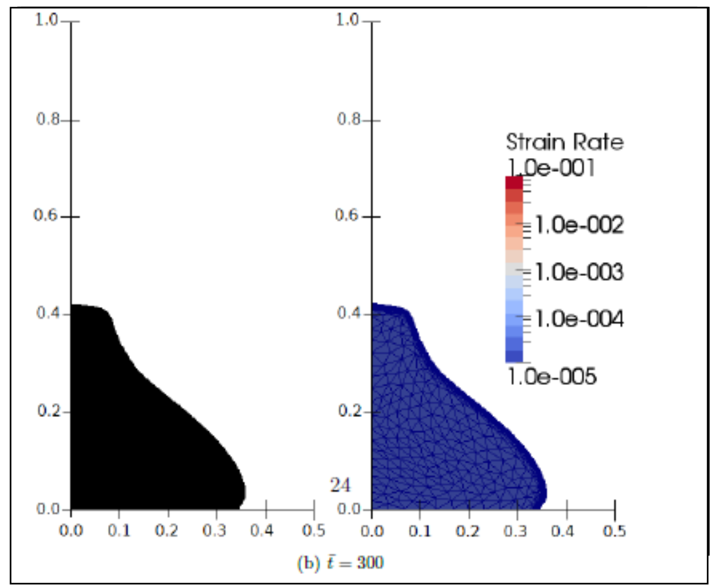

2D and 3D Bingham collapse (a=10) with Bn = 0:1 at t = 1; 100; 200; 300

Numerical test 4: Compressed material (new benchmark)

- Different buckling regime

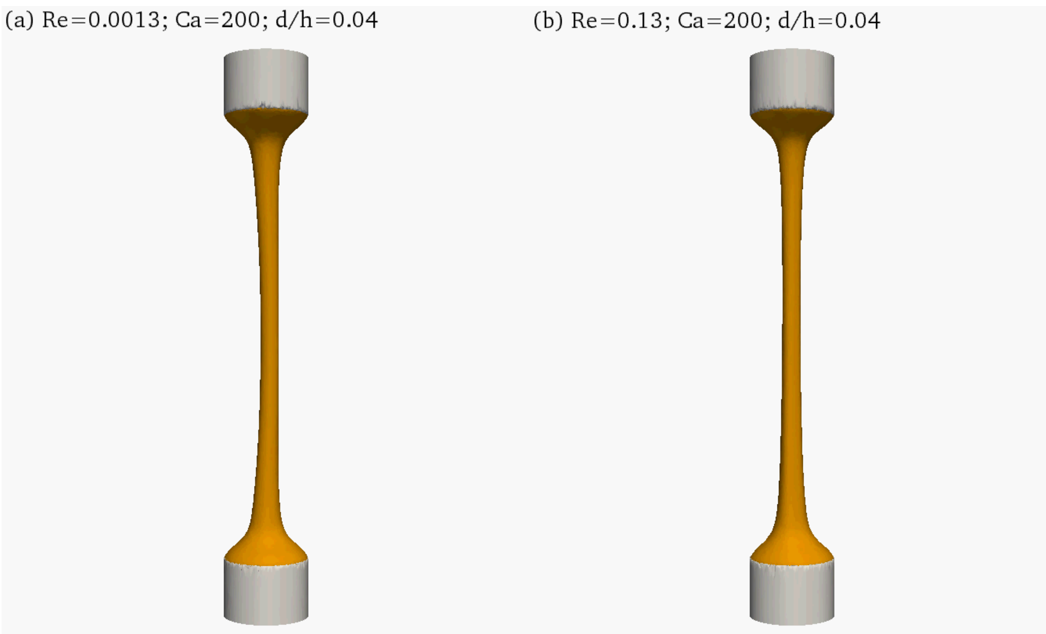

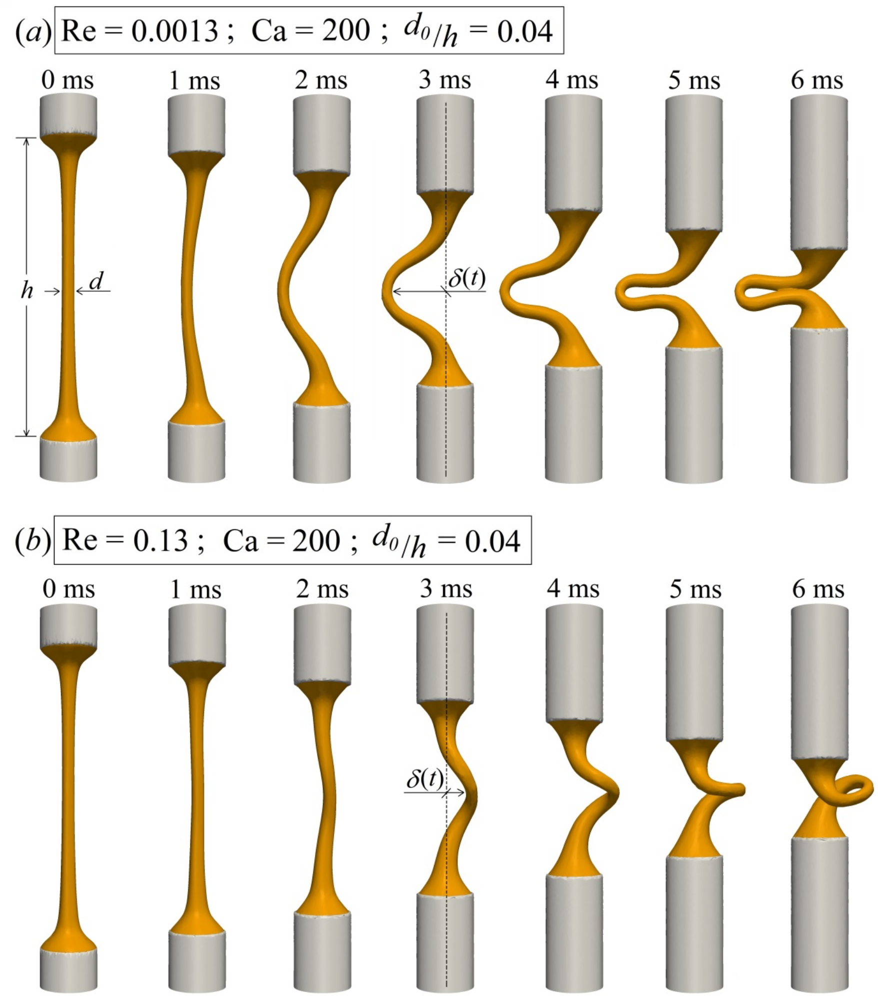

Numerical test 4: Compressed material (new benchmark)

- Main results

Reliable Eulerian Framework

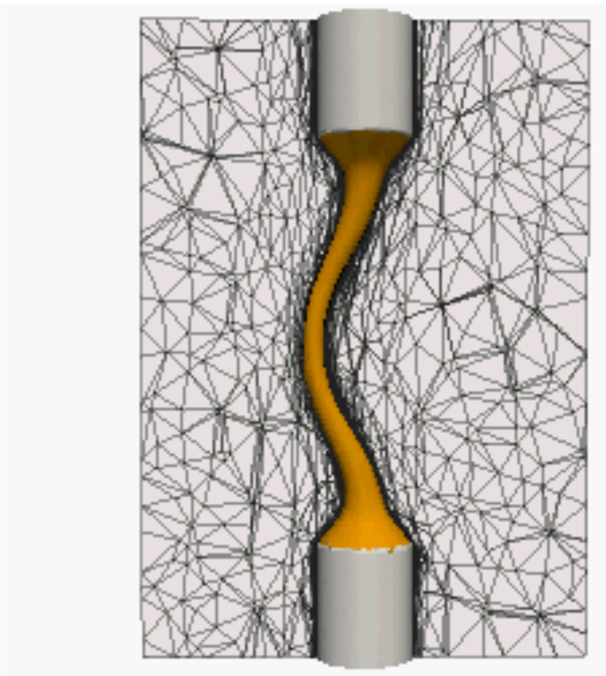

Experimental comparisons

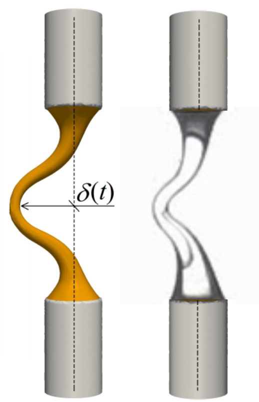

Extensive analysis

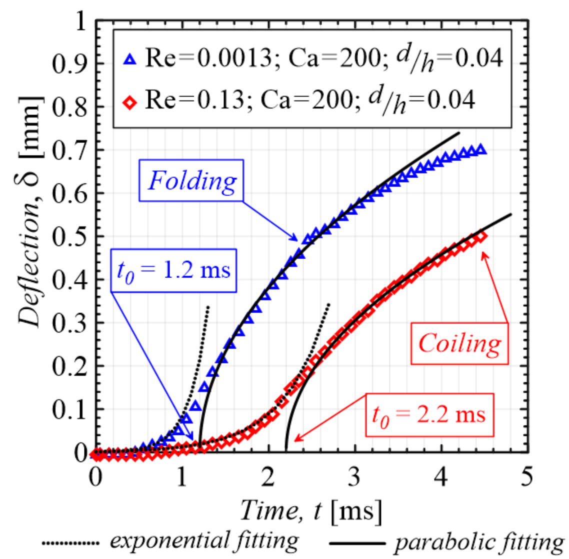

A. Pereira, A. Larcher, E. Hachem, R. Valette, Capillary, viscous, and geometrical effects on the buckling of power-law fluid filaments under compression stresses. Computers & Fluids, 190, 514-519 (2019)

Numerical test 5: Bingham droplet in water (new benchmark)

- Yield stress water-entry: “microfluidic encapsulation”

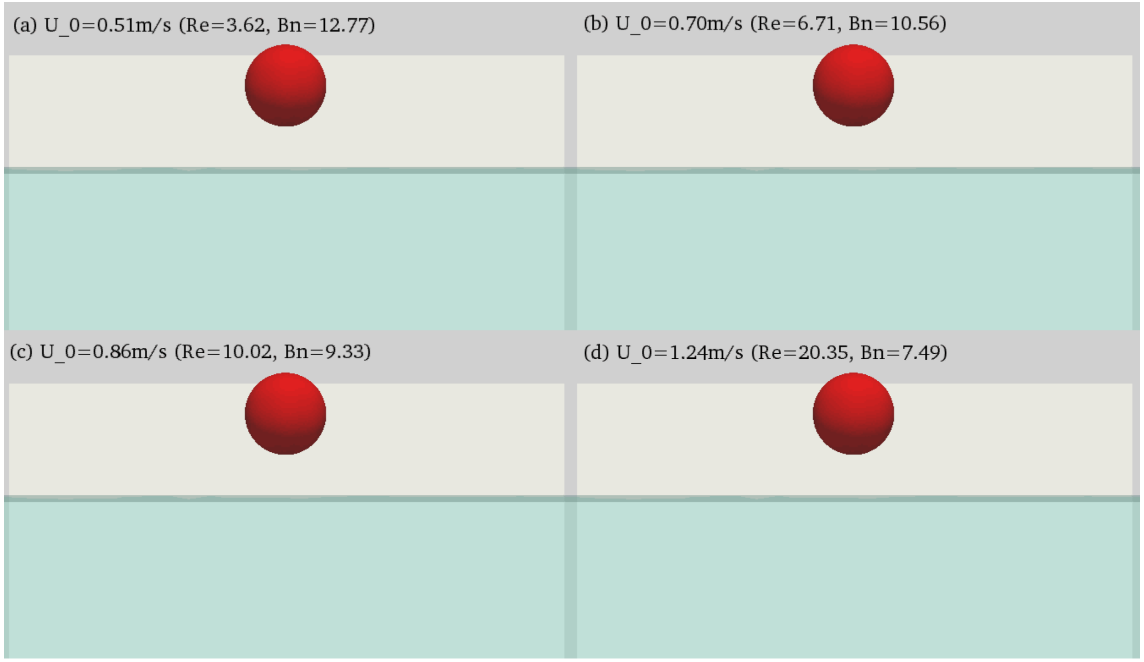

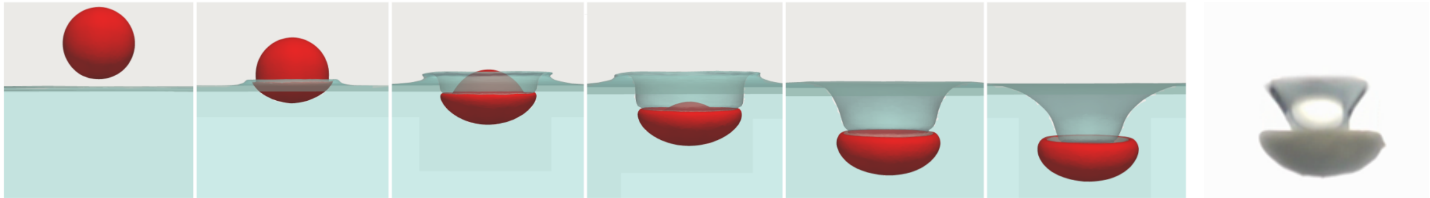

Numerical test 5: Bingham droplet in water (new benchmark)

- Main results: new patent for encapsulation

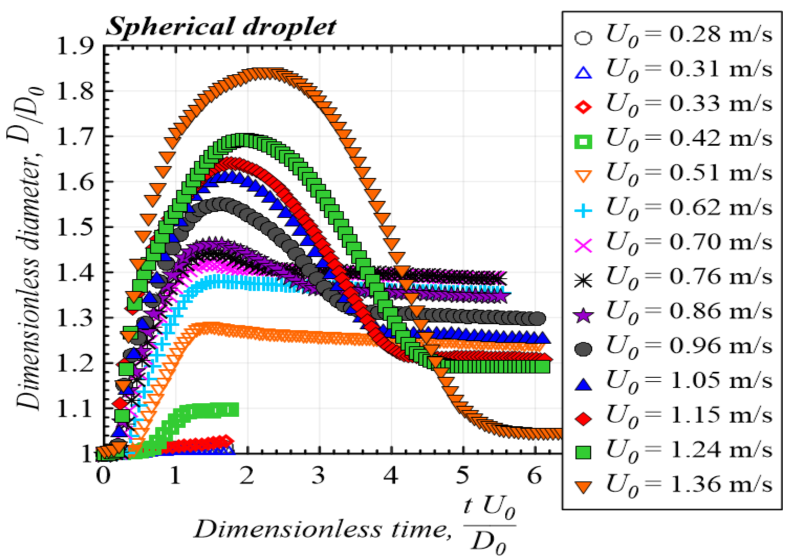

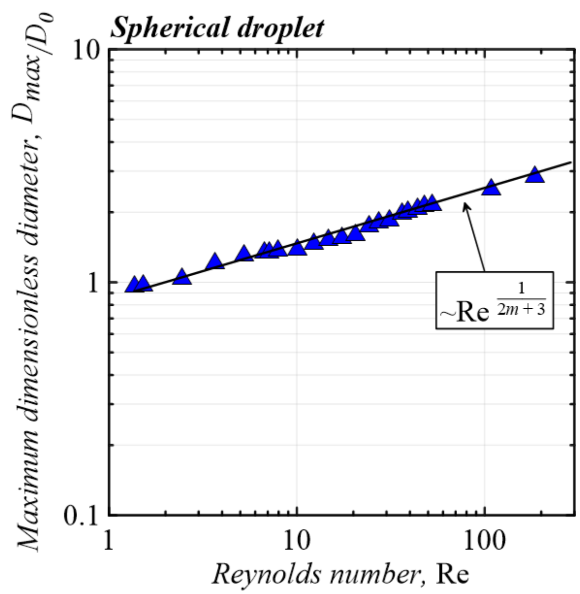

Challenge 1: phase change and boiling

- Thermal threatment in heating furnaces and **quenching tanks**
  - Performed on a material at a solid state
  - To alter its microstructure and properties

- A good thermal threatment :
  - Better quality and availability of products
  - Safer and secured equipments
  - Reduce waste and produce durable materials
  - Avoid repetative manufacturing

- Manufacturing of complex components for the aerospace, aeronautics and automotive industry

Challenge 1: phase change and boiling

- Scheme of the quenching process

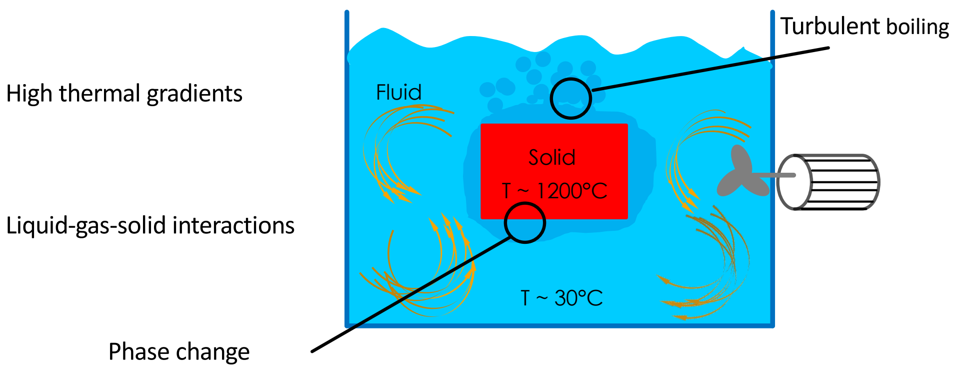

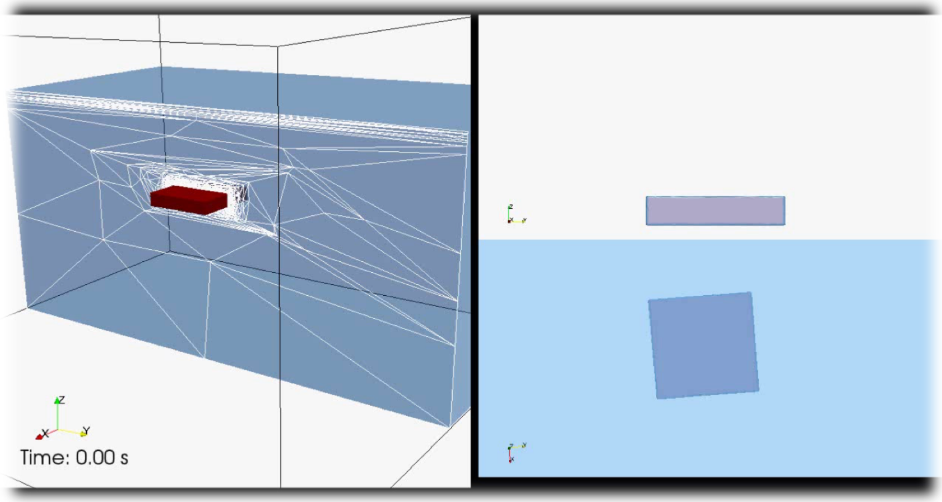

Challenge 1: aid to decision

- Water tank quenching and analysis of the geometry, position, orientation…

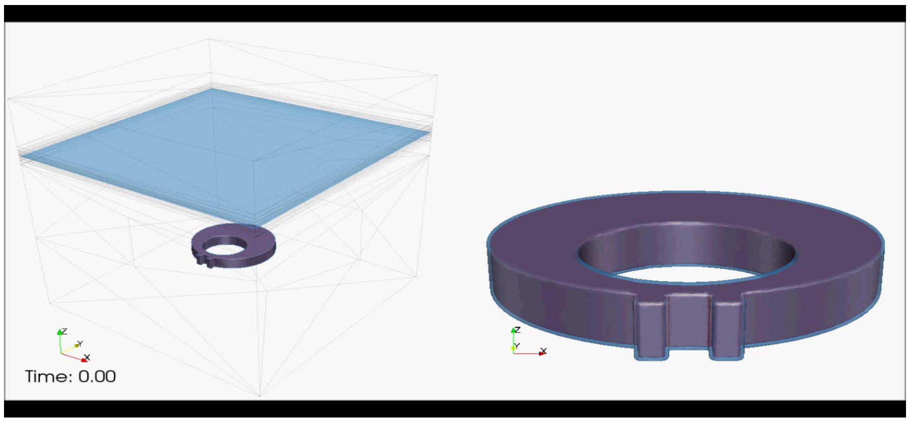

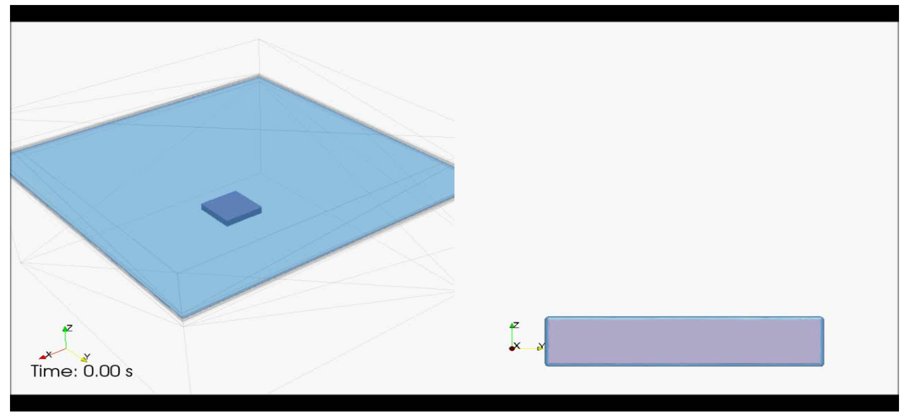

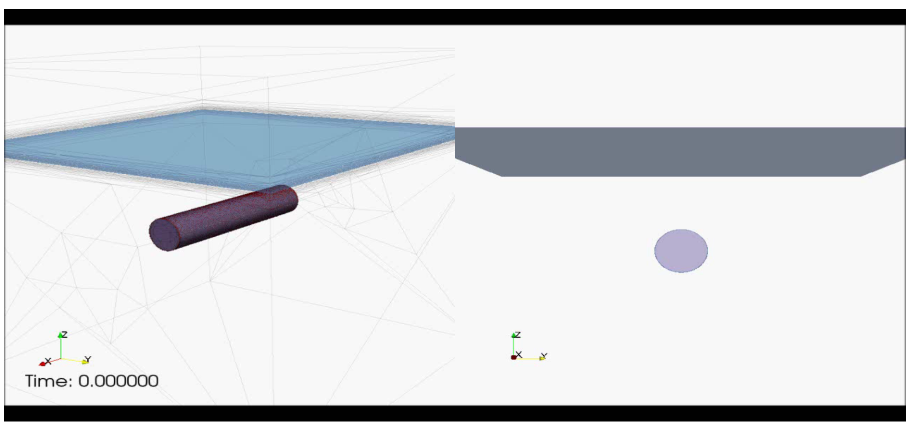

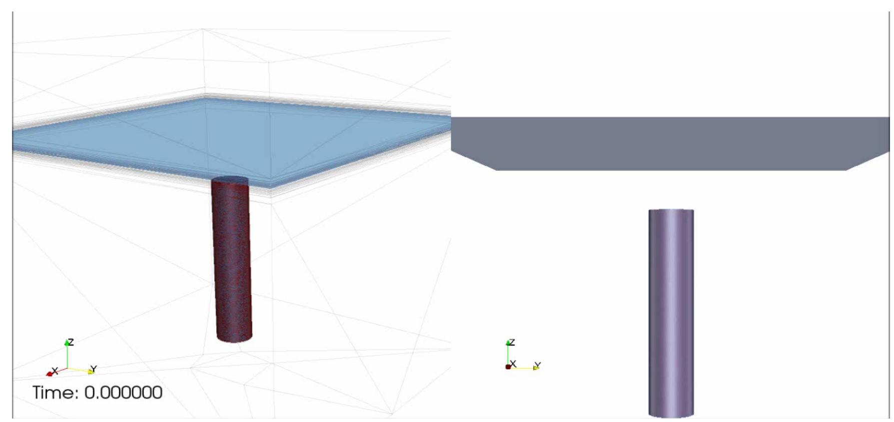

Challenge 2: Jet impinging for cooling

SAFRAN
AIRCRAFT ENGINES

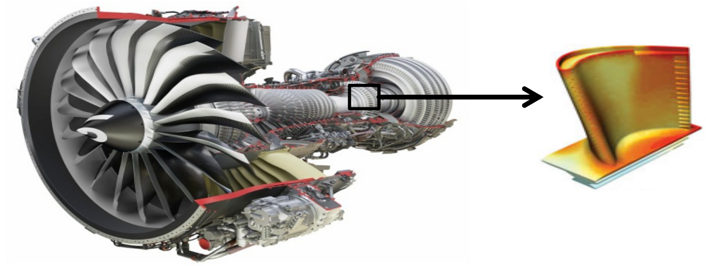

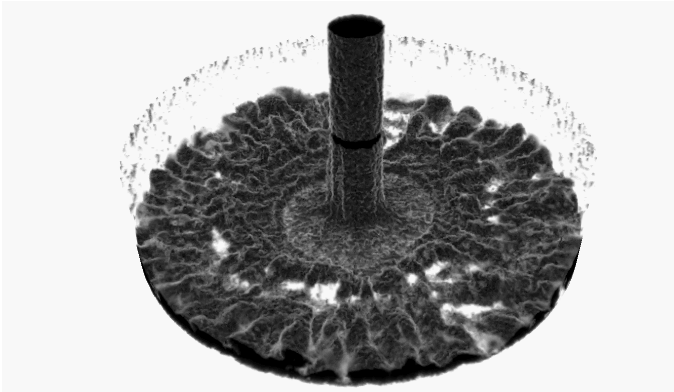

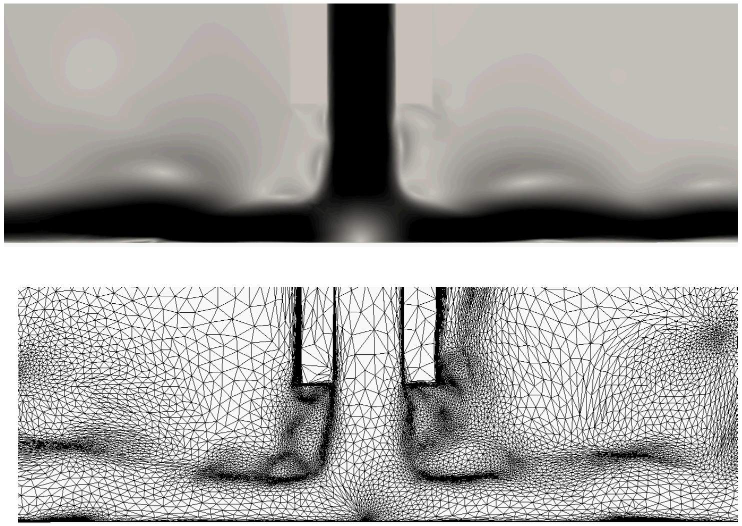

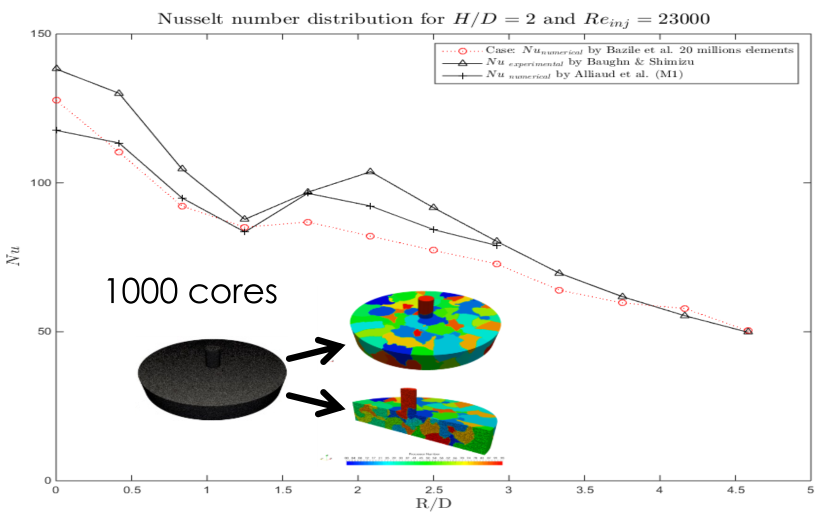

Challenge 3: Aerodynamic performance for a drone and an airship

- SFEM for Spalart–Allmaras turbulence model

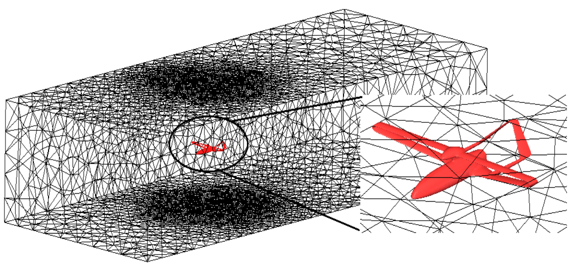

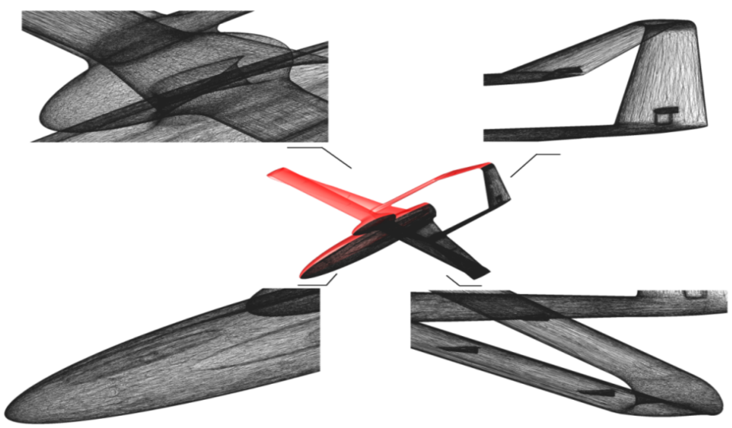

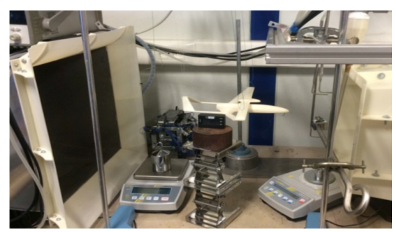

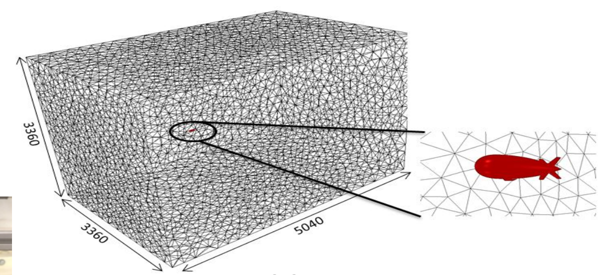

ZOOM

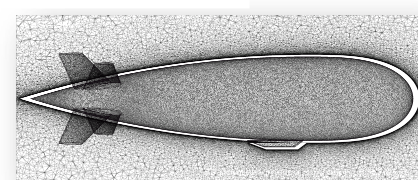

G Guiza, A Larcher, A Goetz, L Billon, P Meliga, E Hachem, Anisotropic boundary layer mesh generation for reliable 3D unsteady RANS simulations, Finite Elements in Analysis and Design 170, 103345, 2020

J Sari, F Cremonesi, M Khalloufi, F Cauneau, P Meliga, Y Mesri, E. Hachem, Anisotropic adaptive stabilized finite element solver for RANS models, International Journal for Numerical Methods in Fluids 86 (11), 717-736, 2018

Challenge 3: Aerodynamic performance for a drone and an airship

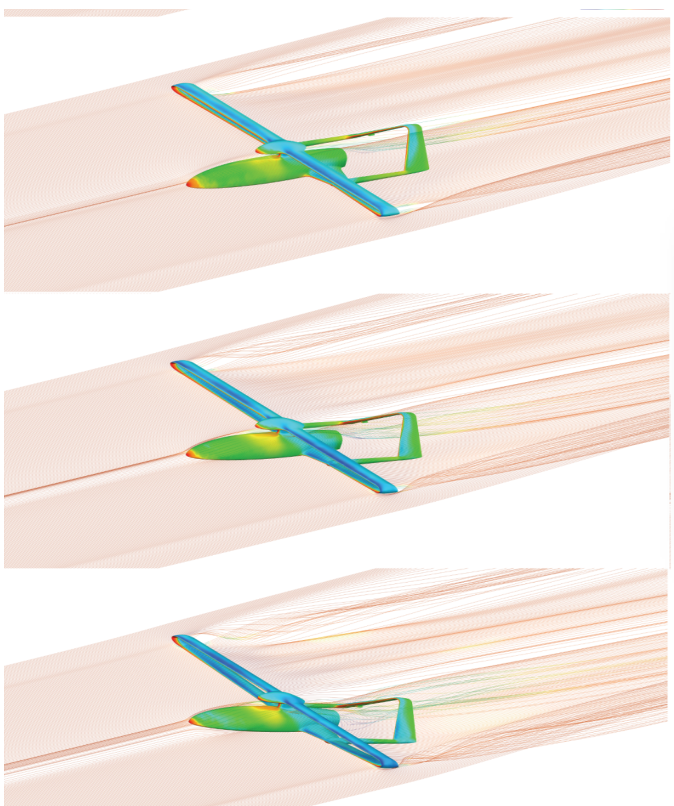

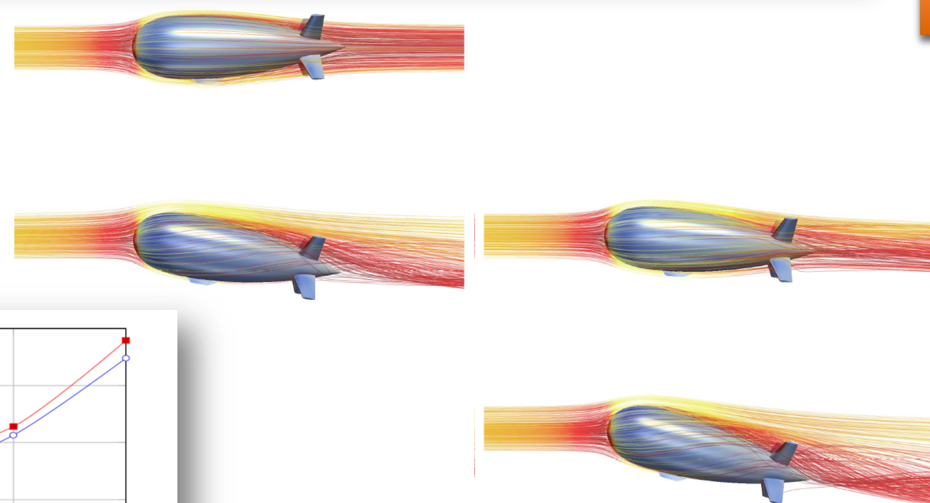

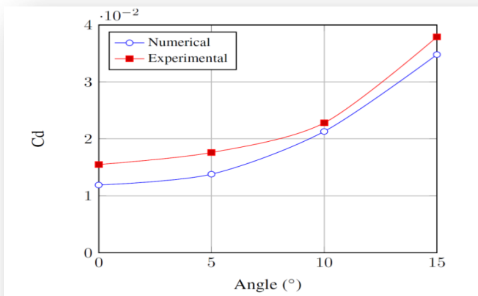

Figure 15. Comparisons for the drag of the UAV at 10m/s

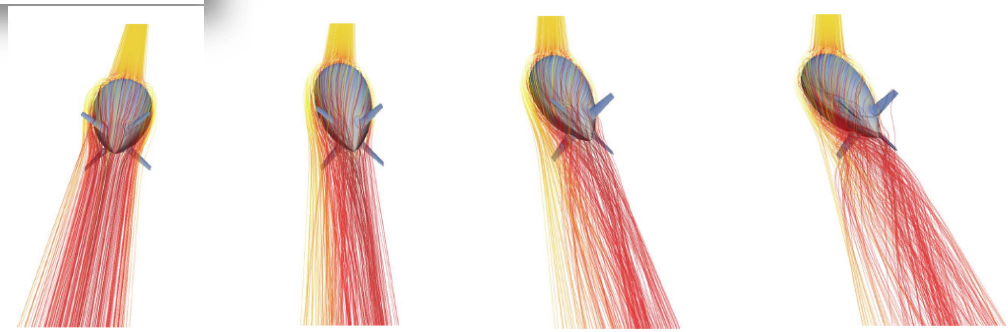

Challenge 4: towards coupling CFD and Data Sciences

Boundary condition

Physical-mathematical model

Velocity field

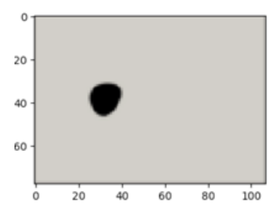

Stationary incompressible Navier-Stokes equations

$$\nabla \cdot \boldsymbol{u} = \boldsymbol{0}$$

$$(\boldsymbol{u} \cdot \nabla)\boldsymbol{u} = -\frac{1}{\rho}\nabla p + \nu \nabla^2 \boldsymbol{u} + \boldsymbol{g}$$

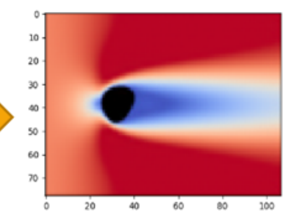

Challenge 4: towards coupling CFD and Data Sciences

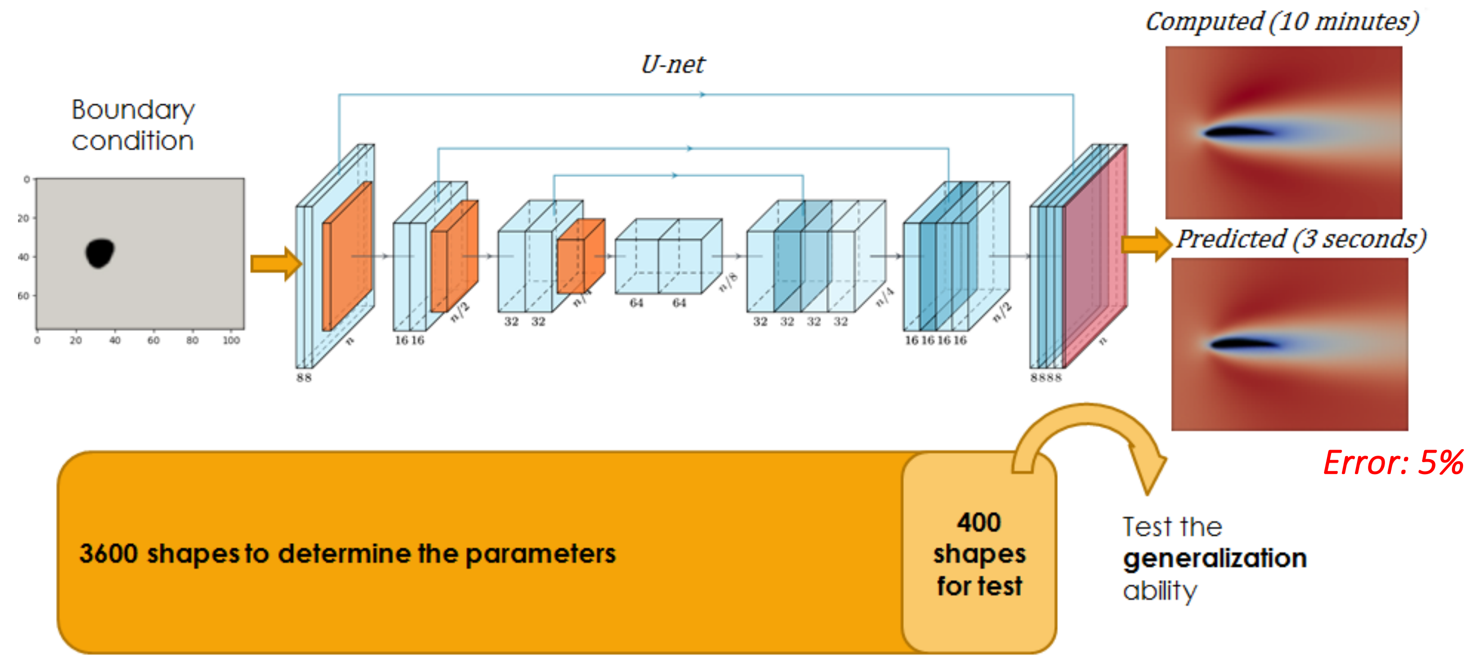

-Jonathan Viquerat, Elie Hachem, *A supervised neural network for drag prediction of arbitrary 2D shapes in low Reynolds number flows*, submitted to Computers & Fluids

Challenge 4: towards coupling CFD and Data Sciences

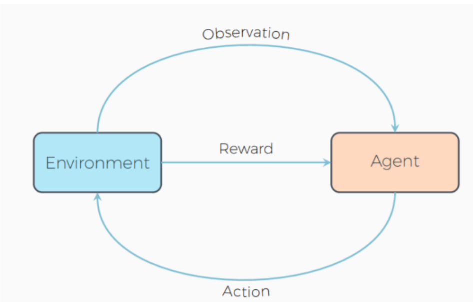

- Shape described with Bezier curves
- Channel domain, inc. N.S.
- Re from 100 to 600
- 3 d.o.f. per point
- Constrained area for each point
- 2 specificities : states and short episodes

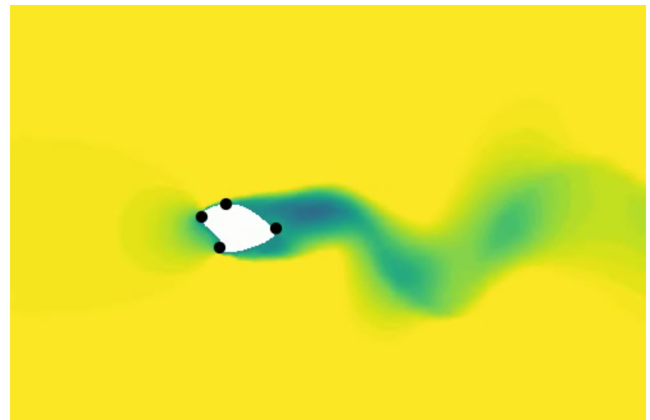

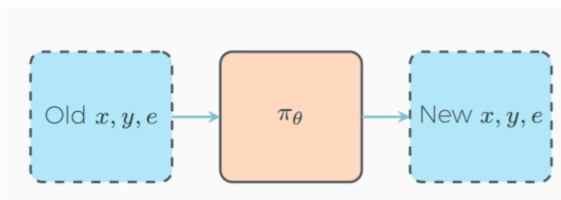

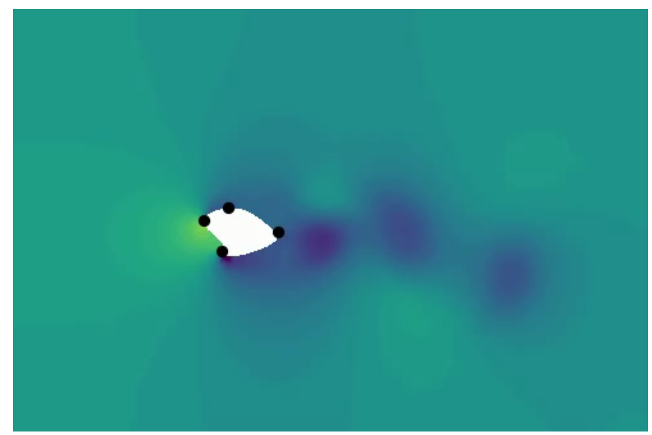

-Jonathan Viquerat, Hassan Ghroueib , Jean Rabault , Alexander Kuhnle,, Aurélien Larcher, Elie Hachem *Direct shape optimization through deep reinforcement learning*, submitted to Journal of Computational Physics

-Paul Garnier, Jonathan Viquerat, Jean Rabault , Aurélien Larcher, Alexander Kuhnle, Elie Hachem, *A review on Deep Reinforcement Learning for Fluid Mechanics*, submitted to Computers & Fluids

Thank you for your attention

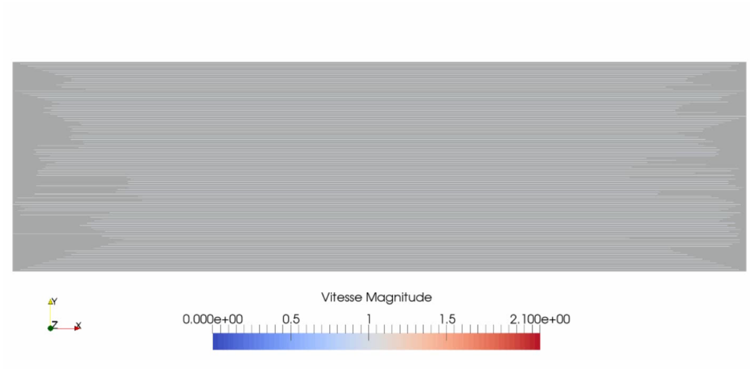

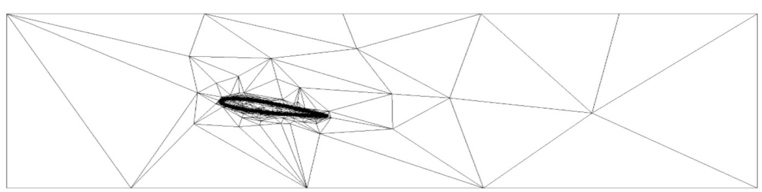

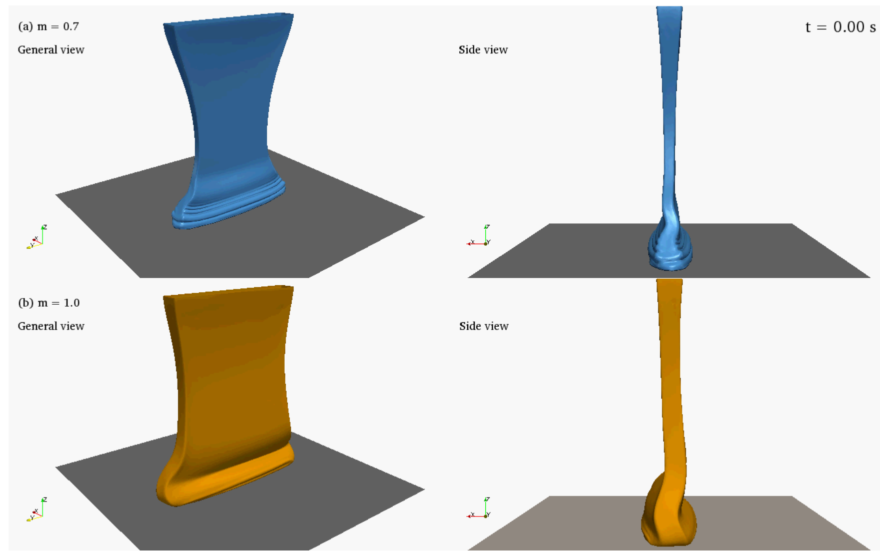

Thanks to all the members of the CFL Research group

elie.hachem@mines-paristech.fr

Conservative interpolation

Ensuring conservation of linear momentum and mass

$$\text{Minimize : } \int_{\Omega_2} |\, \tilde{u}_2 - u_2 \,|^2$$

$$\text{Under the constraints : } \int_{\Omega_2} \tilde{u}_2 = \int_{\Omega_1} u_1$$

$$\int_{\Omega_2} \nabla \cdot \tilde{u}_2 = \int_{\Omega_1} \nabla \cdot u_1$$

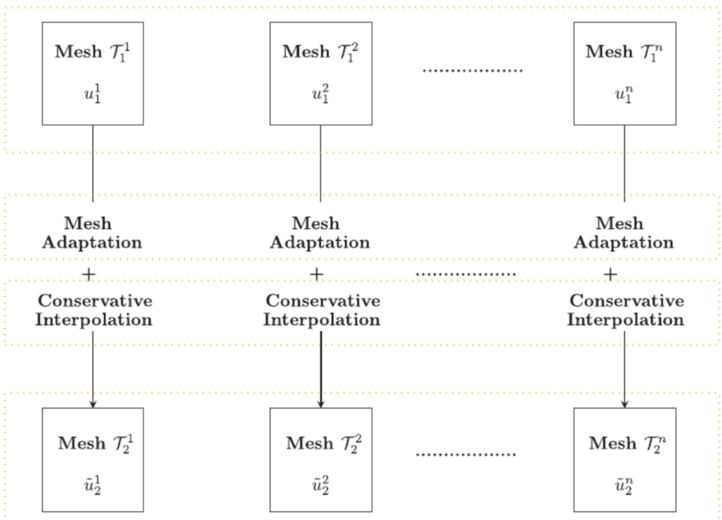

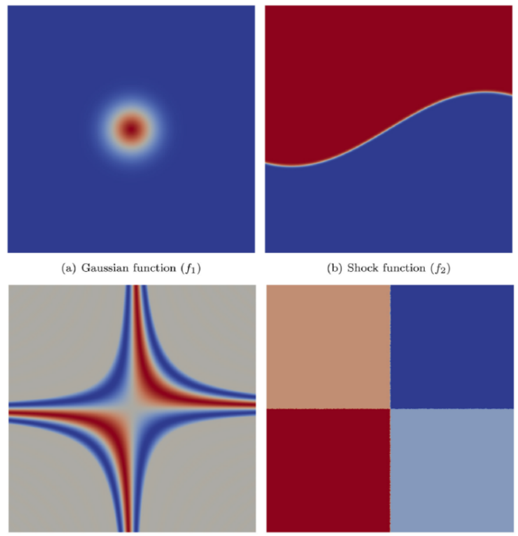

(a) Gaussian function (f_1) (b) Shock function (f_2)

(c) Multiscale function (f_3) (d) Discontinuous function (f_4)

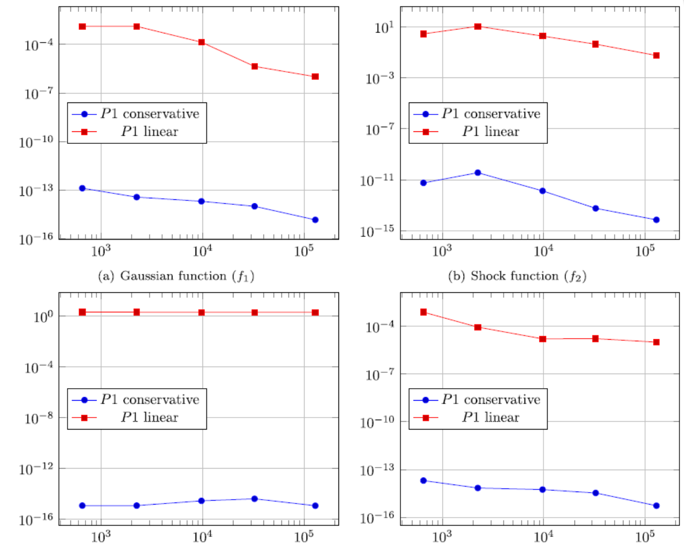

(a) Gaussian function (f_1) (b) Shock function (f_2)

(c) Multiscale function (f_3) (d) Discontinuous function (f_4)

3D meshes used for the different transfers.

Step	Number of nodes in $\mathcal{T}_1^i$	Number of nodes in $\mathcal{T}_2^i$
1	651	587
2	1769	1125
3	39012	29414
4	77941	71778
5	170785	113539